Interim Technical Report
AFSWP – 970
October 1956

TREE BREAKAGE CHARACTERISTICS UNDER STATIC LOADING OF SEVERAL HARDWOOD SPECIES

DIVISION OF FIRE RESEARCH
FOREST SERVICE
U. S. DEPARTMENT OF AGRICULTURE

ACKNOWLEDGMENTS

The author wishes to acknowledge the assistance of W. Lai and F. M. Sauer in their helpful discussions concerning analytical procedures. G. D. Cooper, D. S. Dealey, and S. L. Krugman aided in data reduction.

Agriculture--Forest Service, Berkeley, Calif.

TREE BREAKAGE CHARACTERISTICS UNDER STATIC-LOADING OF SEVERAL HARDWOOD SPECIES

by

W. Y. Pong

Interim Technical Report
AFSWP-970
October 1956

U. S. Department of Agriculture
Forest Service
Division of Fire Research
Washington, D. C.
A. A. Brown, Division Chief

Project Leader: W. L. Fons
California Forest and Range Experiment Station
P. O. Box 245
Berkeley, California

SUMMARY

An investigation was made to determine the energy necessary to cause breakage and uprooting of hardwood trees, and to determine the extent of damage that may occur in a hardwood forest at a given energy level. The analysis presented in this paper delineates essential parameters involved in breakage and uprooting of tree stems by a single load. These parameters provide a basis for the correlation of experimental data.

Twenty-four trees consisting of six species selected from a site II or better mixed-hardwood forest were tested under static loading. Quantitative measures of the force and deflection required to break and uproot these trees were recorded.

Static work modulus values were calculated by use of dimensionless parameters of force, deflection, and restoring force constant derived from the field data for each tree. The results are presented by plotting the actual frequency distributions of the static work moduli by species and type of failure, or both, as percent of cases occurring which are equal to or less than any chosen modulus value. The general level and magnitude of the frequency distributions were found to be approximately the same regardless of species or type of failure. Statistical tests indicate that all the trees tested are from the same population. Therefore, grouping of all static work modulus values into one frequency distribution appears to be justified.

Application of the results of this study should permit the prediction of the energy required to break or uproot any given tree in a site II or better hardwood forest for any probability level. The extent of damage that this forest may sustain for a given energy level may also be predicted.

CONTENTS

TABLES

ILLUSTRATIONS

INTRODUCTION

Wind damage in the form of fallen and broken trees has been studied in both conifer and hardwood forests. The damage was often very heavy and extensive. Anderson (1)[1/] reported damage in Scotland totaling more than 45 million cubic feet of timber after the storm of January 31, 1953. Clapp (5) and Curtis (6) estimated that between 3 and 4 billion board-feet of timber was windthrown in New England by the hurricane of September 21, 1938. Earlier studies of damage were reported by Behre (2), who gave an account of the blowdown in the Adirondacks after the windstorm of 1916, and Cajander (4), who studied the damage caused by a storm which struck Finland in 1933.

Despite the copious amount of literature pertaining to windfall and breakage of trees, very little progress has been made in quantitative determination of the force necessary to cause uprooting and breakage, and of the extent of damage associated with known forces. In his thorough investigation on New England hurricanes, Smith (15) attempted to classify 123 storms according to the intensity of damage which was known to be caused or may have been caused by these storms. Smith acknowledges the fact that the classification was unsatisfactory because of a lack of information on damage and variability in method with which wind velocities were recorded at different localities.

Sherlock et al (14) investigated the variation in strength of transmission poles in relation to the wind forces which act against them. They concluded that the distribution of the windload to the individual poles in the line depended on the relative flexural stiffness of the poles as well as the relative resistance to movement in the ground. Trees may be subjected to similar wind forces as poles, but the reactions of the trees to these forces are quite different because of differences in base fixity. Day (7) in his study on windthrow observed a definite rocking of the tree's root system before it was thrown.

The purpose of this study is to determine 1) the energy necessary to cause breakage and uprooting of hardwoods and 2) the extent of damage that may be expected in a hardwood stand when exposed to different levels of energy.

1/ Underlined numbers in parentheses refer to Literature Cited, page 43.

Previous studies on breakage of conifers by static-loading have been reported by Fons (10) and Sauer et al (13), and from these investigations breakage of conifers was related to known forces and the probability of breakage with given forces could be predicted. The analysis which follows is based on a similar approach using a static work modulus parameter in analyzing the field data.

PROCEDURE

Data for this report were collected in the summer of 1952 from a site class II or better mixed-hardwood forest in the Pisgah National Forest, North Carolina. The elevation of the general area on which trees were tested was approximately 2,300 feet. The species included in this study are given in table 1.

Table 1.--Common and botanical names of test trees

Common name	Key	Botanical name
Yellow-poplar	Y.P.	Liriodendron tulipifera L.
Sweet birch	S.B.	Betula lenta L.
American beech	A.B.	Fagus grandifolia Ehrh.
Pignut hickory	P.H.	Carya glabra Sweet
Silver maple	S.M.	Acer saccharinum L.
Scarlet oak	S.O.	Quercus coccinea Muenchh

Trees were selected on the basis of good stem form, freedom from defects, and vigorous growth. Trees varied in diameter from 6 to 22 inches and in height from 49 to 100 feet.

For each tree selected for testing, total height, diameter at breast height,[2] and position of load application point[3] were measured (figure 6). After the tree was limbed and topped above the loading point, the stem was rigged with cable, and the necessary recording instruments were arranged in a manner shown in figure 1. The general set-up was similar to that used by Fons (10) in his work on conifers

2/ Breast height is 4-1/2 feet above ground level.
3/ Loading point was arbitrarily set at the midpoint of the crown.

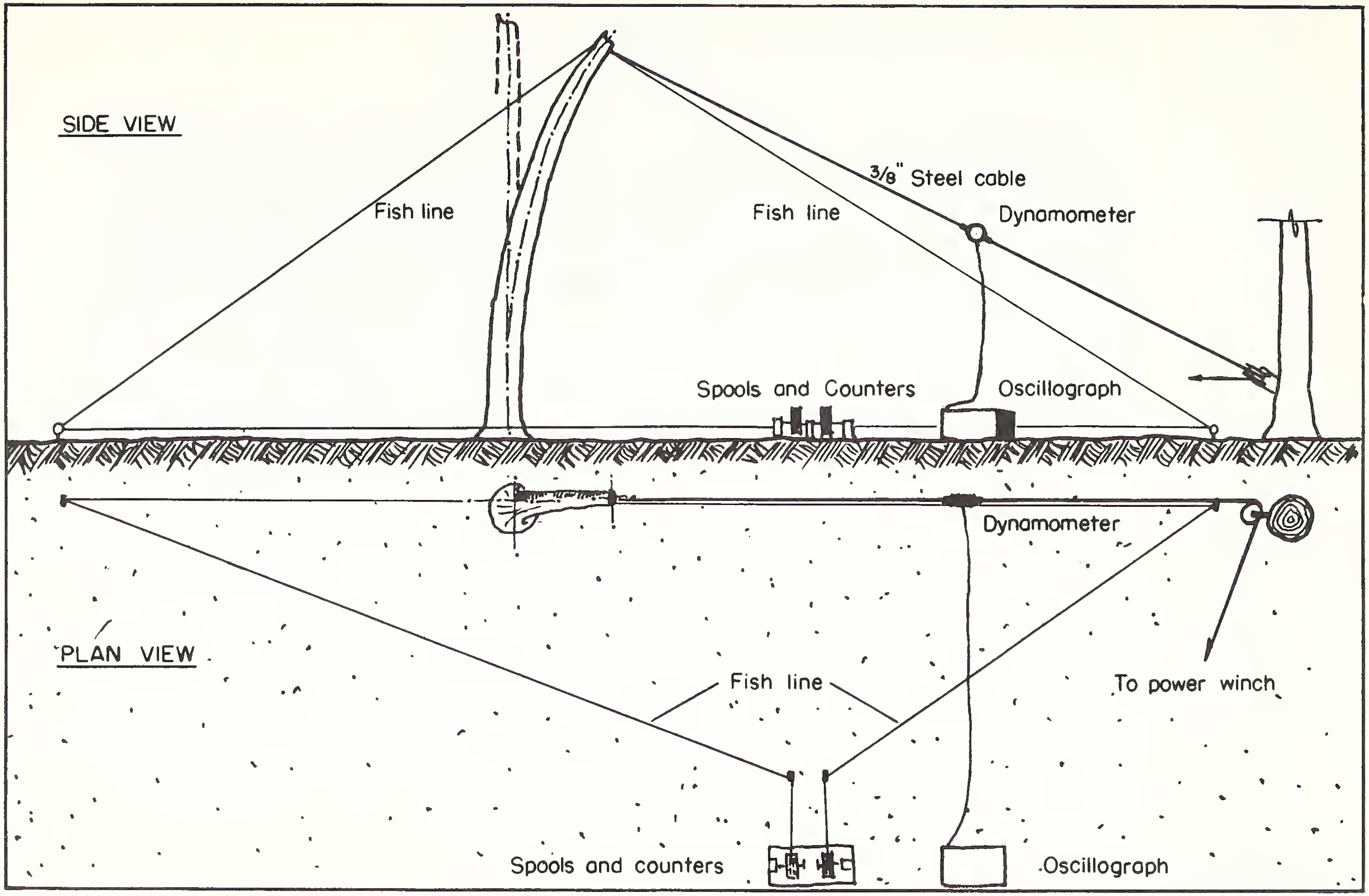

Figure 1.--Layout for static bending test

except for the manner in which the deflection of the loading point was determined. In this study two leads of fish line were attached on opposite sides of the loading point and in the same plane as the cable and central axis of the tree. The lines were held in tension by spring-loaded wooden spools 2 feet in circumference onto which the lines were wound (figure 2). Each spool was connected to a separate counter calibrated to register movement of the loading point in counts equivalent to 1/10 of a revolution of the spool (0.2 ft.).

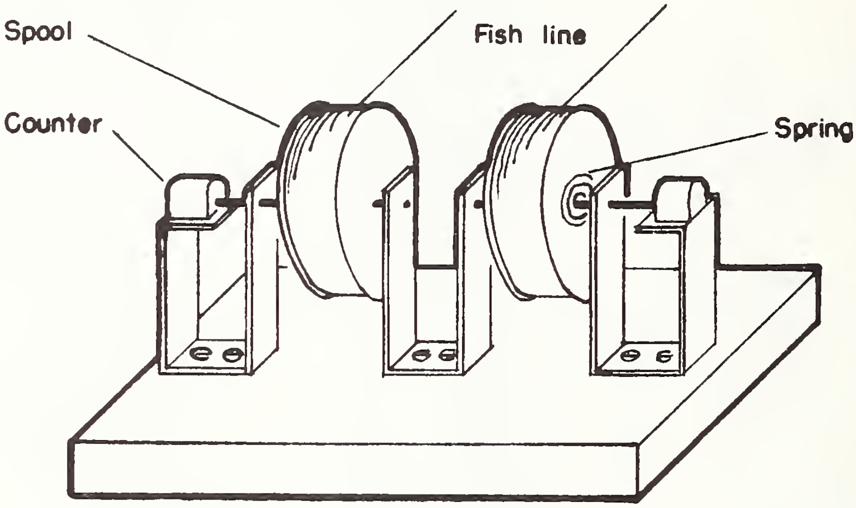

Figure 2.--Spring-loaded spools for loading-point movement determinations in static bending tests

The ring dynamometer (figure 3) and the Sanborn 127 oscillograph used by Fons were also employed in this study for load measurement and recording.

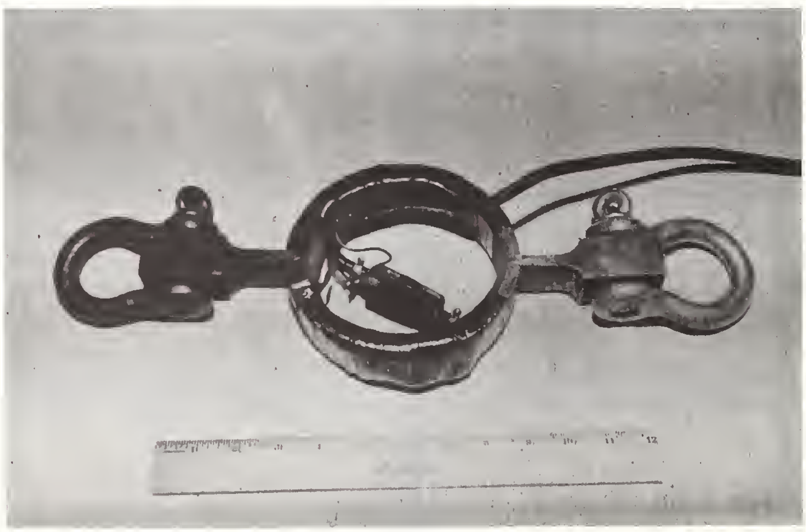

Figure 3.--Ring dynamometer for load measurement

Loading was stopped at successive intervals of 3 to 4 feet deflection at which time the counters were read and the force recorded on the oscillograph. This procedure continued until the stem broke or uprooted (figures 4 and 5). From the series of counter readings, the deflection of the loading point could be plotted by triangulation for correspondingly measured loads.

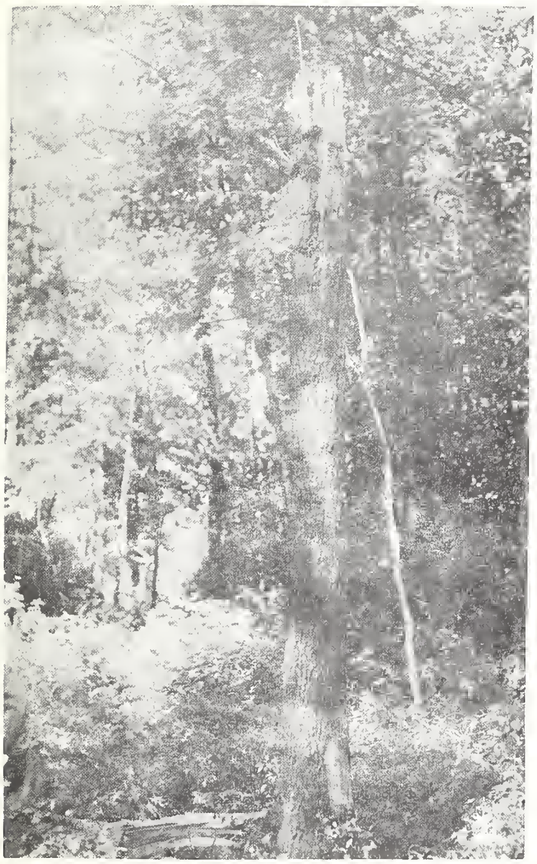

Figure 4.--Typical tree stem break, TB-8, scarlet oak

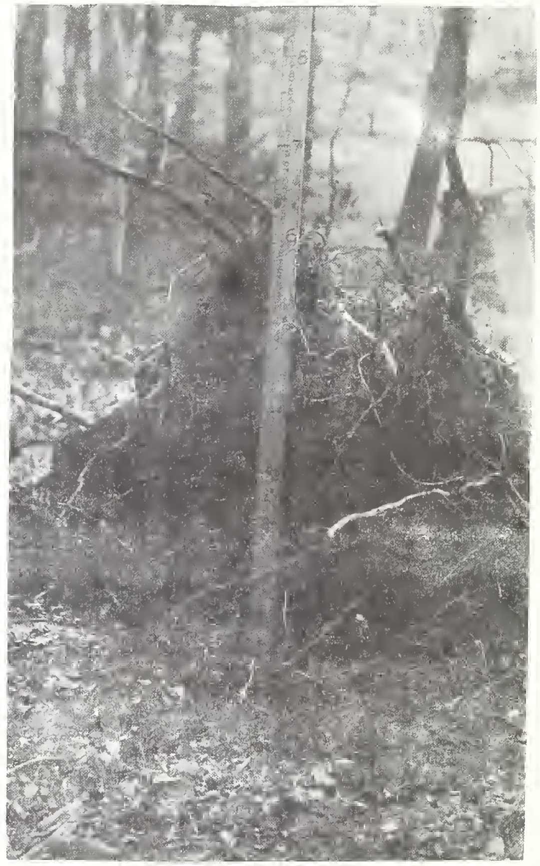

Figure 5.--Uprooted tree stem, TA-38, sweet birch

After the stem failed, cuts were made at stump height,[4/] breast height, below and above the break when breakage occurred, and at convenient intervals along the remaining portion of the stem. Characteristics of the failure were recorded along with its position on the stem, and average diameters inside bark at each cut were measured for determination of form factor.

4/ Stump height is 1 foot above ground level.

DATA AND RESULTS

Table 2 presents data on the physical characteristics of each tree stem tested, grouped according to species. Deflection at failure, and position of loading (figure 6) and of breakage, when breakage occurred, are also presented.

Determination of the force at failure, R_{eb}, required the calculation of an equivalent force acting horizontally at the loading point (figure 7) whose moment at breast height is equal to the moment created by the recorded force R_a. The equivalent force at each interval of deflection and at failure was determined by the equation

$$R_e = \frac{R_a \times L}{H_{cp}} \qquad (1)$$

Figures 8-11 illustrate typical force-deflection curves obtained in this study where the chord deflections at corresponding equivalent forces were measured from plotted points derived from counter readings. In the region where the deflection is proportional to the applied equivalent force the actual restoring force constant, k_a, was determined from these curves. These values are presented in table 2. Force-deflection data for all trees tested are tabulated in Appendix A.

The values of a and b in table 2 are the constants in Behre's (3) stem-form equation

$$z = \frac{f}{af + b} \qquad (2)$$

and were obtained from graphs drawn for each tree similar to the one in figure 12. In drawing the straight line, taper curves (figure 13) were plotted for each tree to serve as guides in weighing those points having the most influence on stem form.

Mechanical properties used for computations were for green wood and are presented in table 3 (11). Table 4 presents a summary of the type of stem failures that occurred for the species tested.

Stem-breakage parameters presented in table 5 were calculated from equations previously derived by Fons (10) and Sauer et al (13) in their conifer breakage reports. Only those equations directly used in determining the various parameters are presented in the text of this study. Reference should be made to the before-mentioned reports for complete derivations.

Table 2.--Experimental stem breakage data[1/]

Column		1	2	3	4	5	6	7	8	9	10	11	12	13	14
Tree No.	Species	Age (yrs)	H_o (ft)	H_{bh} (ft)	H_{cp} (ft)	d_{bh} (in.)	d_i (in.)	b	a	c	f_1	R_{eb} (lb)	y_b (ft)	k_a (lb/ft)	f_{br}
TA-14	Y.P.	33	69.1	64.6	39.0	6.1	5.5	.510	.590	.864	.404	253	37.2	10.2	.96
TA-29	Y.P.	32	77.8	73.3	41.5	8.3	7.8	.580	.500	1.160	.434	353	28.9	36.7	.84
TA-34	Y.P.	60	100.1	95.6	53.7	21.6	19.5	.545	.650	.838	.442	3,920	16.7	450.0	
TA-35	Y.P.	46	85.9	81.4	37.5	10.5	9.5	.555	.580	.957	.542	895	23.0	68.0	.97
TA-37	Y.P.	50	94.8	90.3	53.0	14.6	13.2	.660	.460	1.435	.420	1,367	26.0	72.9	.82
TA-23	S.B.	53	78.6	74.1	44.0	12.5	11.8	.560	.530	1.057	.406	2,062	16.6	183.6	.78
TA-31	S.B.	67	61.5	57.0	31.5	13.7	13.0	.850	.208	4.087	.451	3,142	12.6	608.8	
TA-38	S.B.	56	71.4	66.9	40.0	11.2	10.5	.632	.463	1.365	.402	1,273	23.3	138.0	
TA-39	S.B.	63	53.6	49.1	22.9	6.0	5.4	.668	.452	1.478	.534	383	20.2	63.0	
TA-44	A.B.	51	48.5	44.0	25.8	5.9	5.8	.665	.350	1.900	.414	524	21.1	38.0	.87
TA-45	A.B.	62	61.3	56.8	32.6	9.6	9.2	.685	.365	1.877	.426	1,208	19.1	103.6	
TA-22	P.H.	59	77.0	72.5	51.9	9.9	9.0	.520	.710	[illegible]	.299	2,117	43.1	46.3	
TA-23	P.H.	52	59.3	54.8	30.8	7.9	7.0	.400	1.000	.400	.438	379	36.6	26.4	
TA-24	S.M.	58	62.7	58.2	35.3	14.0	13.0	.523	.587	.891	.399	2,812	19.7	325.0	
TA-8	S.O.	64	73.9	69.4	34.3	11.2	10.5	.525	.605	.868	.512	1,994	21.1	267.5	.88
TA-9	S.O.	64	82.1	77.6	52.1	14.3	13.2	.505	.600	.842	.329	2,395	21.8	327.5	.85
TB-1	S.O.	118	84.5	80.0	40.9	14.1	13.2	.410	.780	.526	.489	1,449	20.8	385.0	
TB-2	S.O.	62	79.9	75.4	43.0	11.9	11.1	.580	.520	1.115	.430	1,525	23.3	135.0	
TB-3	S.O.	60	70.6	66.1	30.4	8.2	8.1	.555	.555	1.000	.546	1,387	28.6	94.6	
TB-4	S.O.	61	71.2	66.7	39.4	10.9	10.0	.530	.575	.922	.441	1,115	39.4	76.7	
TB-5	S.O.	58	73.1	68.6	39.6	9.5	8.8	.385	.770	.500	.431	1,773	42.8	98.3	1.00
TB-6	S.O.	49	68.7	64.2	30.5	8.8	8.0	.400	.825	.485	.542	1,286	24.8	136.0	.95
TB-8	S.O.	67	69.8	65.3	38.3	12.1	10.0	.720	.505	1.426	.413	1,981	30.4	131.3	.89
TB-9	S.O.	58	79.3	74.8	45.9	13.8	12.5	.425	.940	.452	.386	3,320	34.2	162.9	.90

1/ Nomenclature given on page 45.

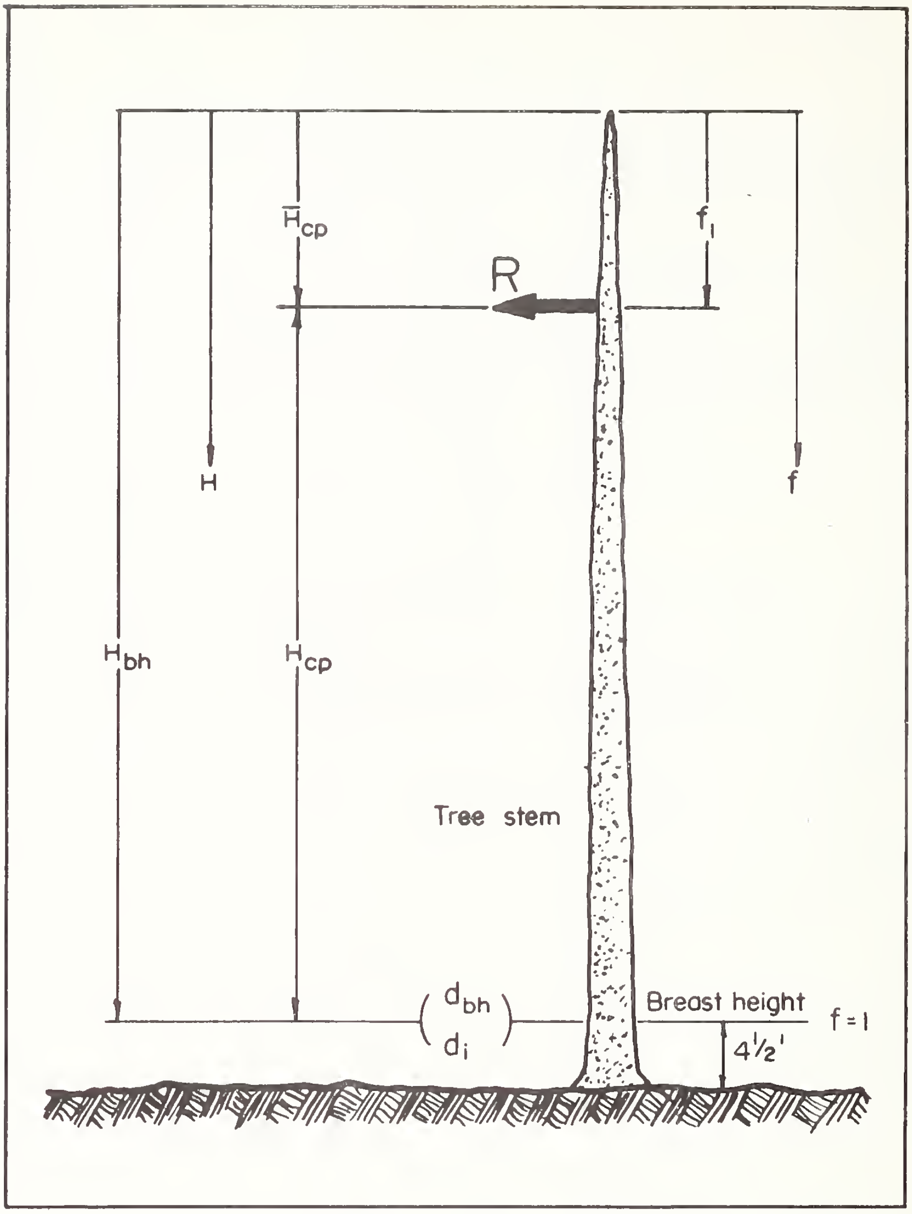

Figure 6.--Schematic diagram of tree stem and associated parameters, nomenclature, page 45

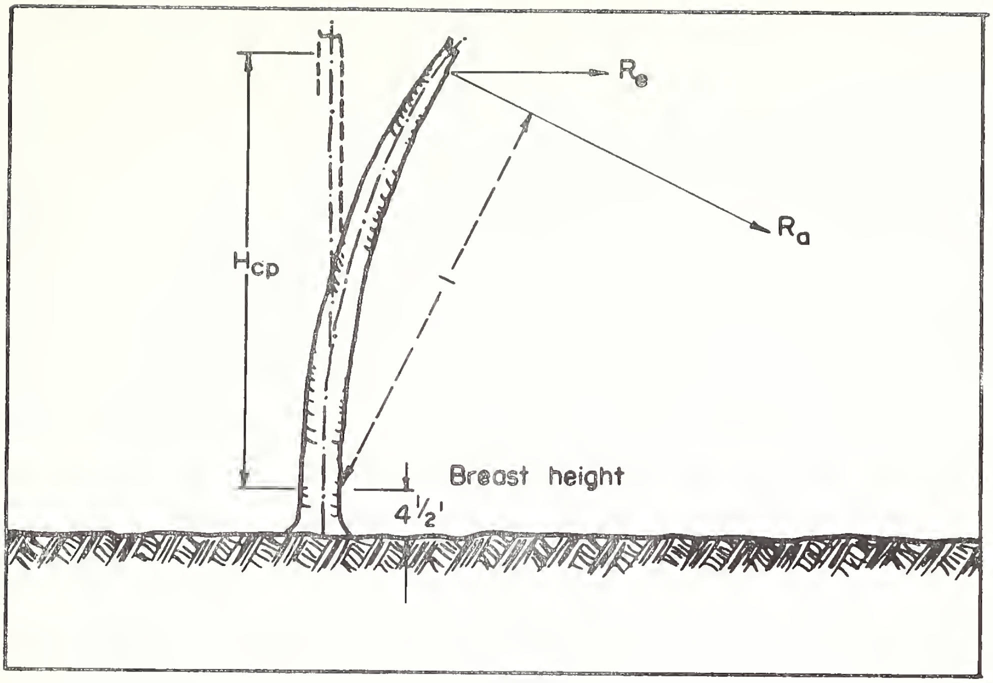

Figure 7.--Equivalent force $R_e = \frac{R_a L}{H_{cp}}$

Table 3.--Mechanical properties of green wood[1/]

Species	Modulus of Elasticity, E (lbs/sq.in.)	Modulus of Rupture, MR (lbs/sq.in.)	Reference Strain δ_r = MR/E x 10^6 (μ in./in.)[2/]
Yellow-poplar	1,090 x 10^3	5,400	4,930
Sweet birch	1,650 x 10^3	9,400	5,700
American beech	1,380 x 10^3	8,600	6,330
Pignut hickory	1,650 x 10^3	11,700	7,210
Silver maple	940 x 10^3	5,800	6,170
Scarlet oak	1,480 x 10^3	10,400	7,060

1/ From (11).

2/ Reference strain values are averaged calculated values for localities cited in the reference.

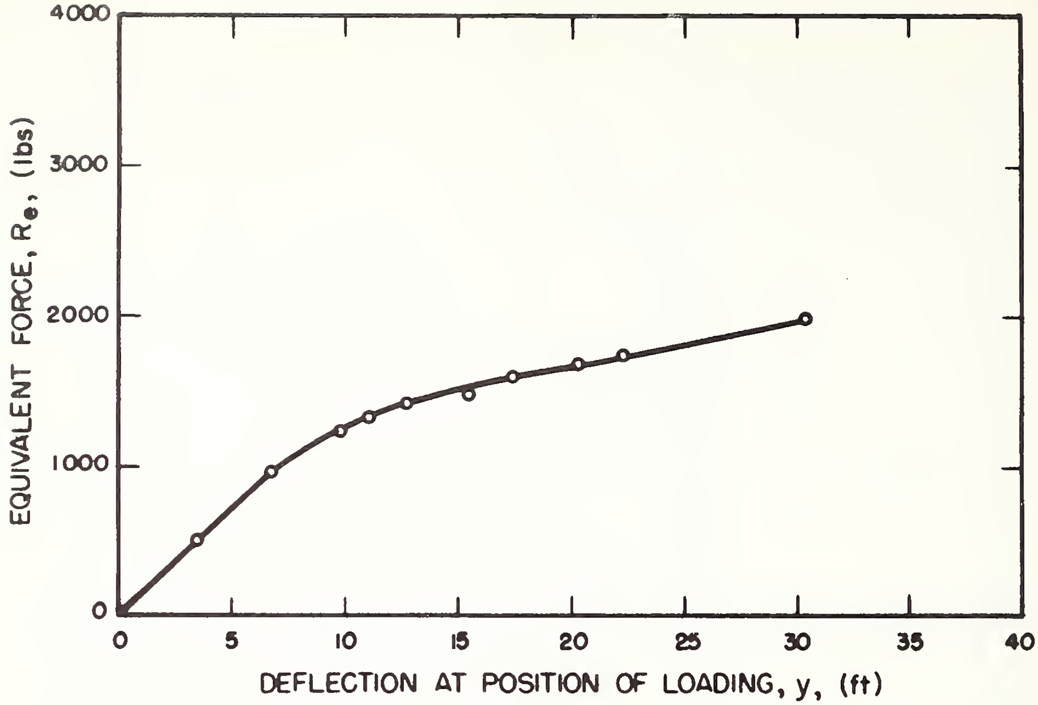

Figure 8.--Force-deflection curve for tree stem No. TB-8, scarlet oak--break

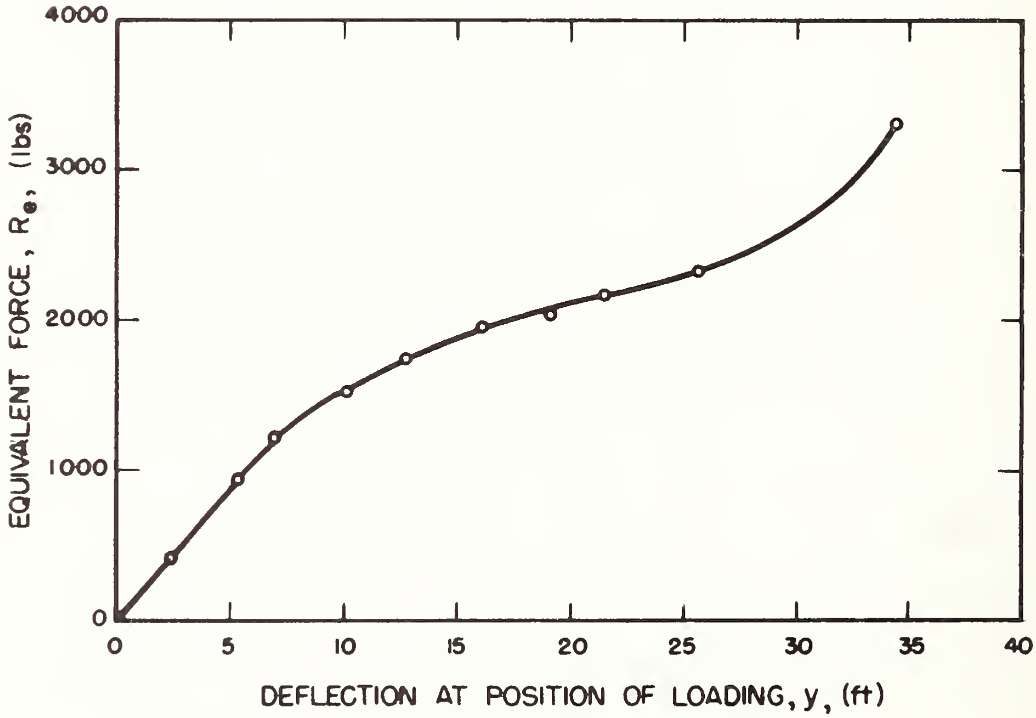

Figure 9.--Force-deflection curve for tree stem No. TB-9, scarlet oak--break

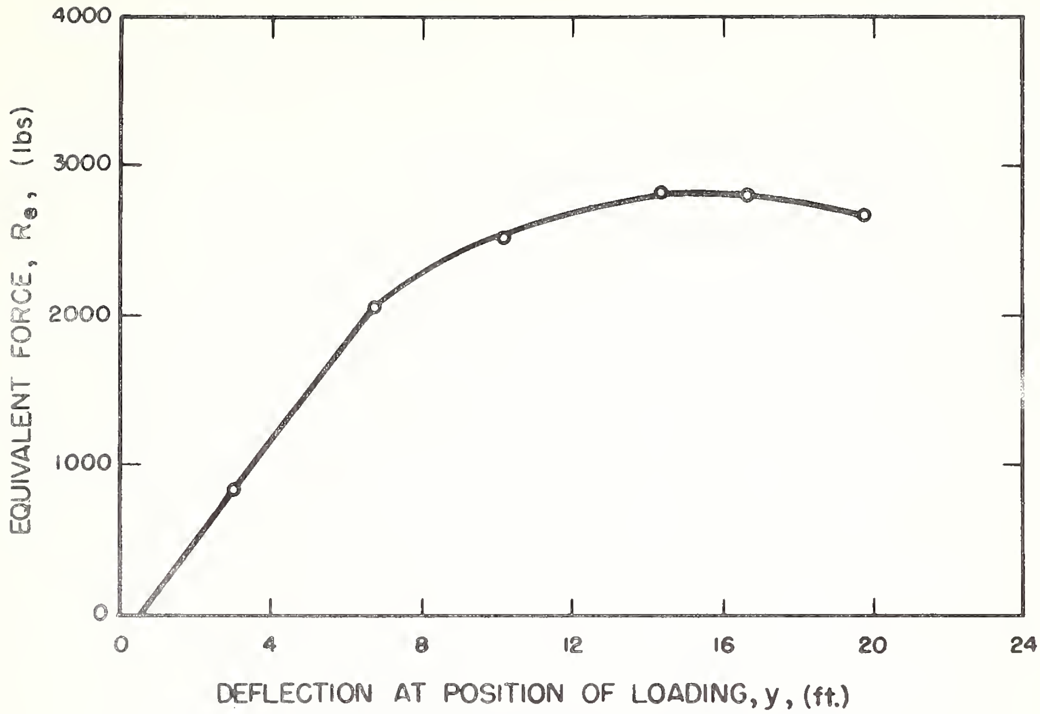

Figure 10.--Force-deflection curve for tree stem No. TA-24, silver maple--uproot

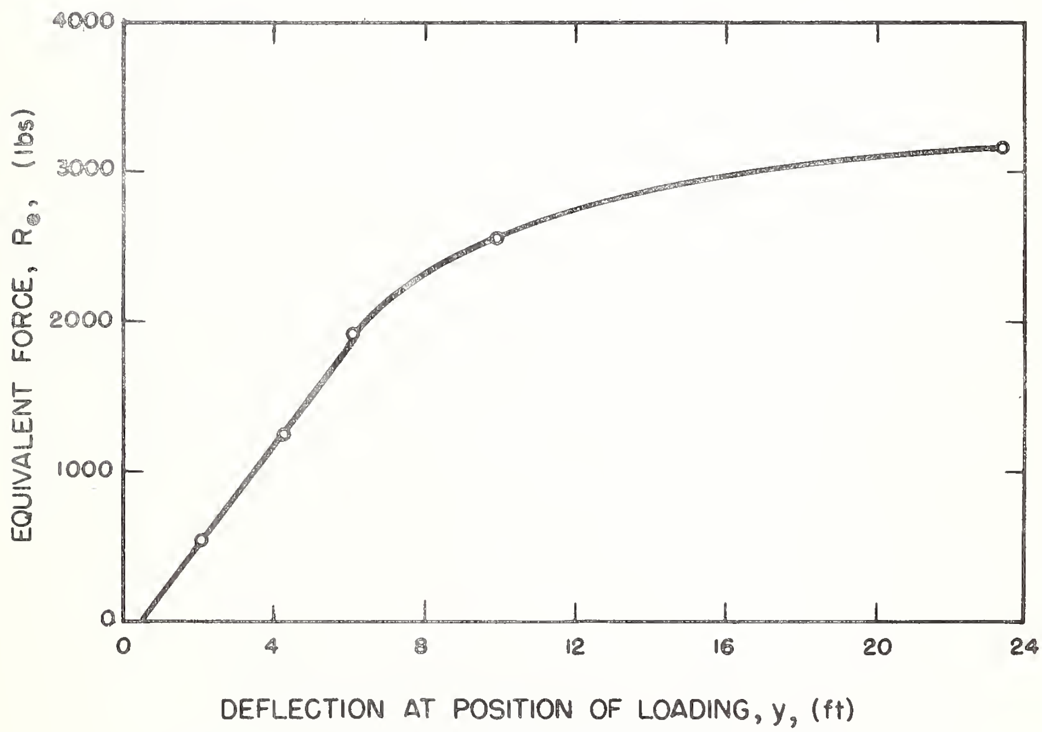

Figure 11.--Force-deflection curve for tree stem No. TA-38, sweet birch--uproot

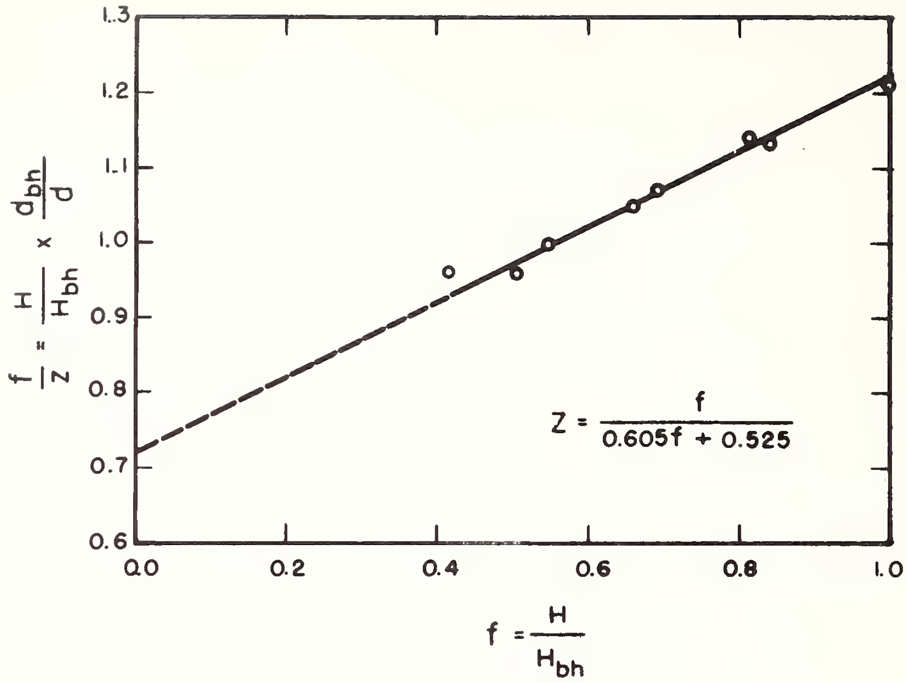

Figure 12.--Plot of z/f as a function of f for tree No. TB-8, scarlet oak

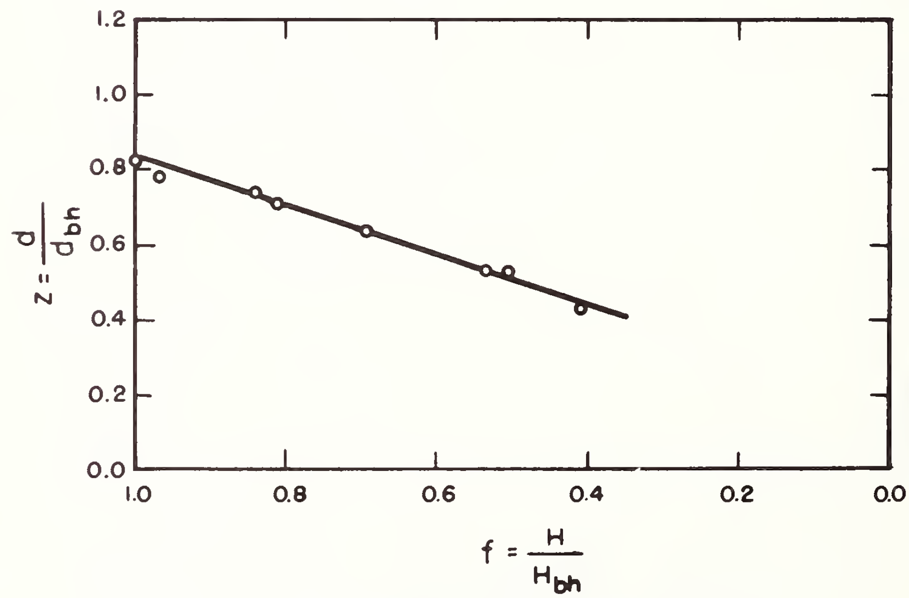

Figure 13.--Taper curve for tree No. TB-8, scarlet oak

Table 4.--Summary of static bending results on hardwoods

Species	Type		
	Break	Uproot	Total
Yellow-poplar	4	1	5
Sweet birch	1	3	4
American beech	1	1	2
Pignut hickory	0	2	2
Silver maple	0	1	1
Scarlet oak	6	4	10
Total	12	12	24

The theoretical restoring force constant, k_r, was determined from the equation

$$k_r = \frac{\bar{\beta}\ 3Ed_i 4\pi}{H^3_{bh}\ 64} \tag{3}$$

Values of $\bar{\beta}$, the restoring force function which contains the theoretical constant k_r, were obtained from a plot of the dimensionless expression

$$\frac{k_r\ H^3_{bh}\ 64}{3E\ \pi d_i^4} = \psi\ (c, f_1) \tag{4}$$

for applicable ranges of c and f_1 (figure 14). Dividing the actual restoring force constant, k_a (table 2) by k_r resulted in the dimensionless restoring force modulus, $\bar{K}$.

Stress along the stem was obtained from the equation

$$\frac{S}{S_{bh}} = \frac{(f - f_1)(f + c)^3}{(1 - f_1)(1 + c)^3 f^3} \tag{5}$$

where

$$S_{bh} = \frac{32R_{eb}\ H_{bh}}{\pi d_i^3}\ (1 - f_1) \tag{6}$$

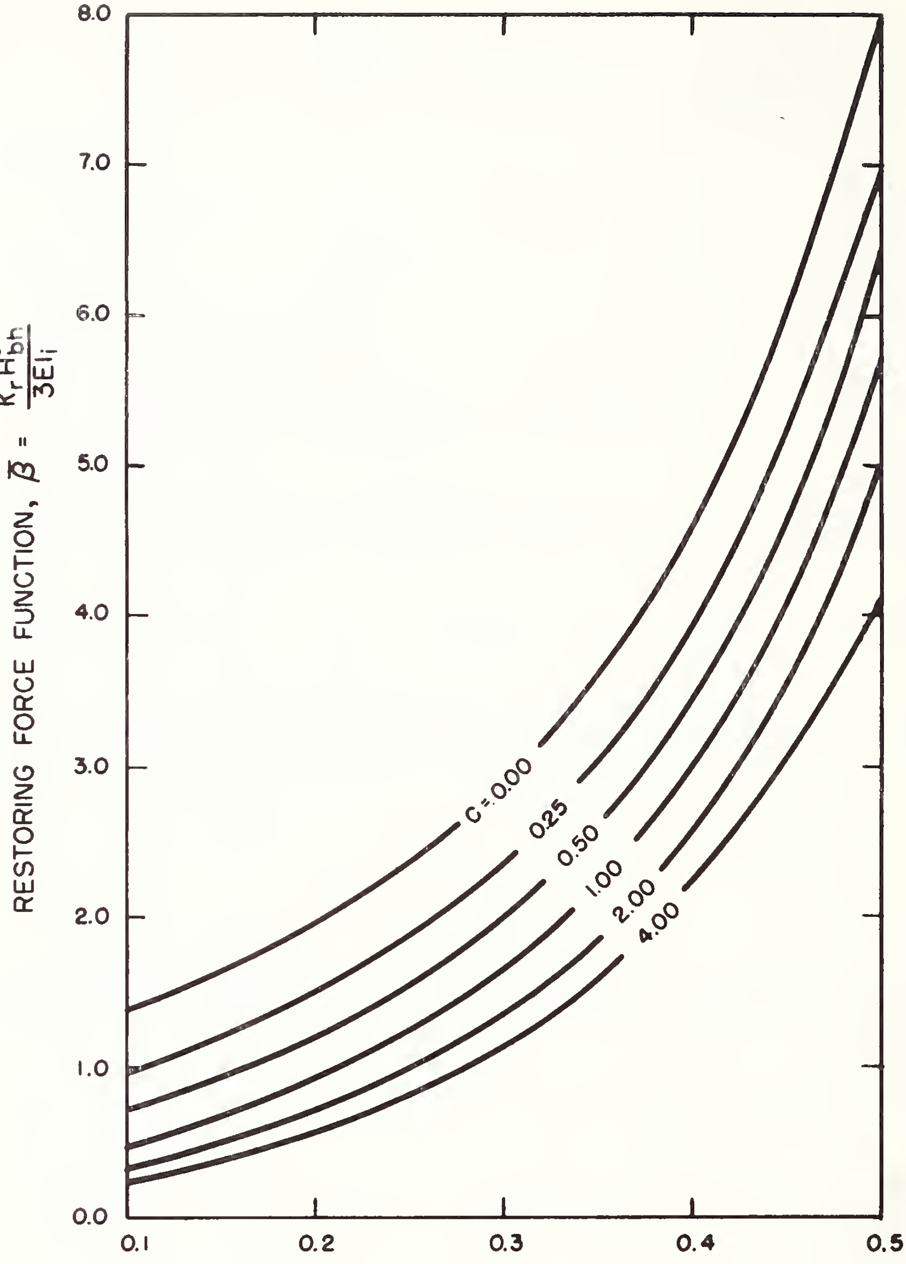

Figure 14.--Dimensionless expression containing restoring force constant, k_r, as a function of position of loading, f_1, and stem form factor, c

Table 5.--Values of derived stem breakage parameters[1/]

Column		1	2	3	4	5	6	7	8	9	10	11	12	13	14
Tree No.	Species	$\overline{\beta}$	k_r (lb/ft)	$\overline{K}$	S_m/S_{bh}	S_{bh} (lb/sq in.)	f_m	S_m (lb/sq in.)	S_{br} (lb/sq in.)	δ_m/y (in./in. / in.)	y_r (ft)	$\overline{Y}_b$	$\overline{R}_r$ (lb)	$\overline{R}_b$	$\overline{E}_b$
TA-14	Y.P.	3.172	11.97	.852	1.000	7,151	1.000	7,151	7,080	26.29	15.62	2.384	187	1.351	1.712
TA-29	Y.P.	3.613	37.97	.967	1.000	3,787	1.000	3,787	3,645	30.93	13.28	2.189	504	0.701	1.035
TA-34	Y.P.	3.993	736.78	.611	1.000	3,450	1.000	3,450	-	49.85	8.24	2.036	6,071	0.645	.957
TA-35	Y.P.	7.373	124.53	.546	1.000	473	1.000	473	463	50.73	8.10	2.839	1,009	0.887	1.965
TA-37	Y.P.	3.123	143.56	.508	1.001	3,825	0.932	3,829	3,787	30.94	13.28	1.954	1,906	0.717	.937
TA-23	S.B.	3.110	254.14	.722	1.000	6,749	1.000	6,749	6,409	41.34	11.49	1.443	2,920	0.706	.696
TA-31	S.B.	3.036	789.48	.711	1.154	5,478	0.745	6,300	-	80.70	5.89	2.135	4,650	0.676	1.153
TA-38	S.B.	2.843	194.74	.709	1.003	4,956	0.899	4,971	-	41.66	11.40	2.044	2,220	0.573	1.078
TA-39	S.B.	6.421	77.84	.809	1.000	6,800	1.000	6,800	-	69.87	6.80	2.972	529	0.725	1.920
TA-44	A.B.	2.841	53.69	.708	1.039	8,466	0.782	9,021	8,683	54.01	9.77	2.168	524	0.998	1.268
TA-45	A.B.	3.061	169.17	.612	1.030	6,183	0.816	6,368	-	53.75	9.82	1.945	1,660	0.727	.942
TA-22	P.H.	1.836	53.28	.869	1.000	18,051	1.000	18,051	-	23.44	25.63	1.683	1,366	1.550	1.146
TA-33	P.H.	4.489	109.79	.240	1.000	4,165	1.000	4,165	-	61.26	9.81	3.734	1,077	0.352	1.283
TA-24	S.M.	3.056	424.68	.765	1.000	5,493	1.000	5,493	-	74.10	6.94	2.838	2,947	0.945	1.999
TA-8	S.O.	6.430	353.88	.756	1.000	7,117	1.000	7,117	6,476	72.17	8.15	2.604	2,884	0.691	1.403
TA-9	S.O.	2.051	221.05	1.477	1.000	6,642	1.000	6,642	6,512	31.44	18.71	1.165	4,136	0.579	.645
TB-1	S.O.	5.998	538.40	.715	1.000	2,533	1.000	2,533	-	65.88	8.93	2.337	4,808	0.301	.641
TB-2	S.O.	3.523	189.24	.713	1.000	5,873	1.000	5,873	-	40.86	14.46	1.618	2,736	0.557	.628
TB-3	S.O.	7.481	169.14	.559	1.000	9,570	1.000	9,570	-	66.44	8.86	3.250	1,499	0.925	2.116
TB-4	S.O.	3.962	201.61	.380	1.000	5,089	1.000	5,089	-	54.79	10.74	3.682	2,165	0.515	1.774
TB-5	S.O.	4.192	117.81	.834	1.000	12,431	1.000	12,431	12,431	47.14	12.48	3.424	1,470	1.206	2.126
TB-6	S.O.	8.041	188.88	.720	1.000	8,989	1.000	8,989	8,401	77.24	7.62	3.263	1,439	0.894	2.086
TB-8	S.O.	3.157	170.66	.769	1.003	9,297	0.910	9,325	9,233	45.37	12.97	2.344	2,213	0.895	1.571
TB-9	S.O.	3.258	286.66	.568	1.000	9,544	1.000	9,544	8,920	46.53	12.64	2.714	3,625	0.916	1.475

1/ Nomenclature given on page 45.

Using Q_{f_1} in place of $\left(\frac{32R_{eb} H_{bh}}{\pi d_i^3}\right)_{f_1}$ and combining the two equations gives an expression

$$\frac{S}{Q_{f_1}} = \frac{(f - f_1)(f + c)^3}{(1 + c)^3 \quad f^3} \tag{7}$$

From this expression stress distribution curves were determined and plotted for each tree stem tested. Typical curves are presented in figure 15.

The position of maximum stress in the stress distribution curve was found by the equation

$$f_m = c - (c^2 - 3cf_1)^{1/2} \tag{8}$$

The ratio of the maximum stress (S_m) to stress at breast height (S_{bh}) was computed for each stem by substituting values of f_m in equation (5). Multiplying the stress at breast height calculated from equation (6) by the stress ratio, resulted in numerical values of the maximum stress, S_m.

For the 12 trees that broke, stress at position of breakage was found by the equation

$$S_{br} = Q_{f_1} \times \left(\frac{S}{Q_{f_1}}\right)_{br} \tag{9}$$

Values of $\left(S/Q_{f_1}\right)_{br}$ were determined from the stress distribution curves at position f_{br}.

Maximum strain per unit of deflection at f_1 was calculated from the equation

$$\frac{\delta_m}{y} = \frac{3d_i \; H_{cp} \; \bar{\beta} \times 10^6}{2H_{bh}^3 \times 144} \times \frac{S_m}{S_{bh}} \tag{10}$$

Substituting values of δ_m/y into the equation

$$y_r = \frac{\delta_r}{\delta_m/y \times 12} \tag{11}$$

resulted in reference deflection values for the different trees tested.

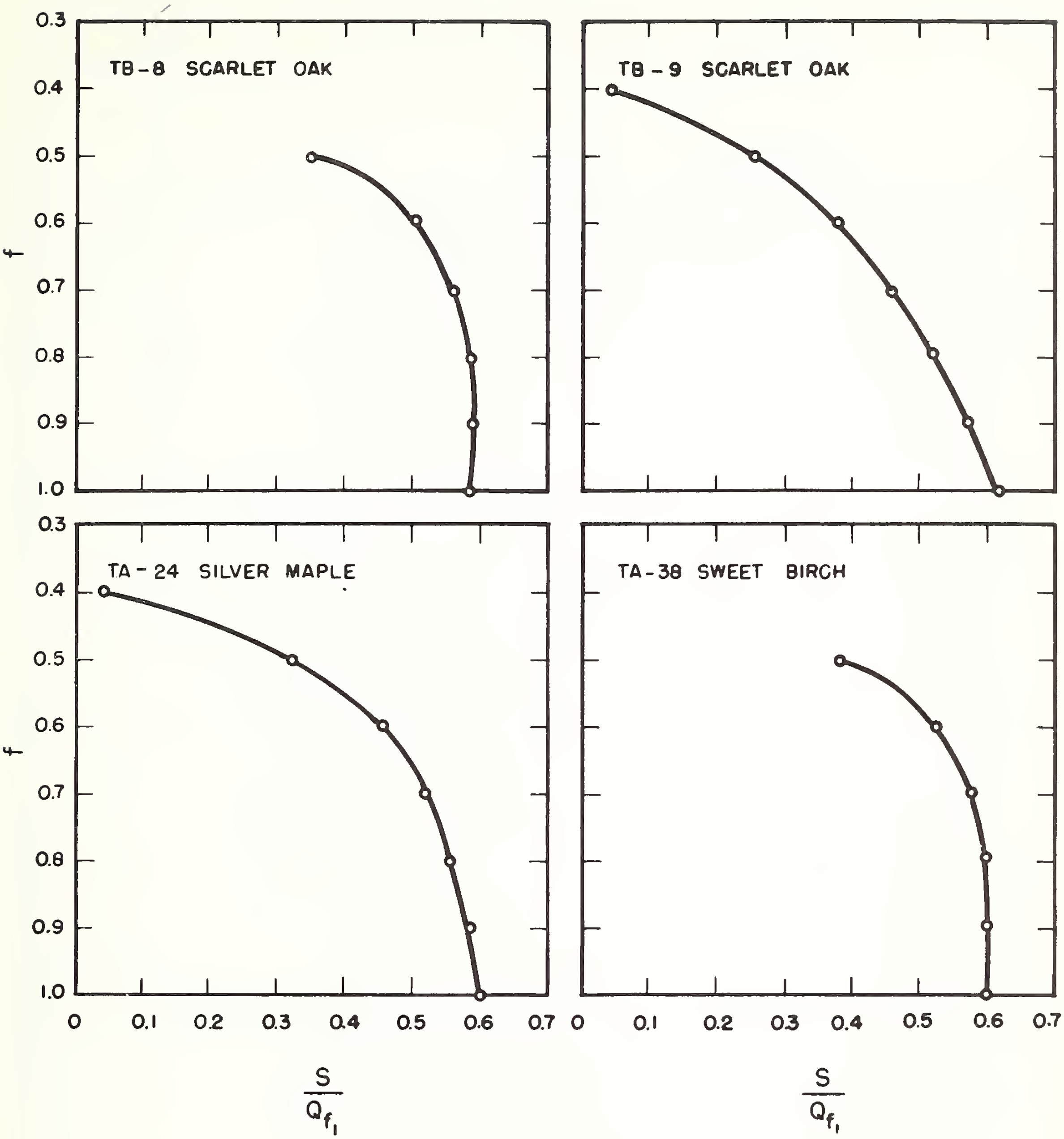

Figure 15.--Typical stress distribution curves at failure for trees breaking (TB-8 and TB-9) and trees uprooting (TA-24 and TA-38)

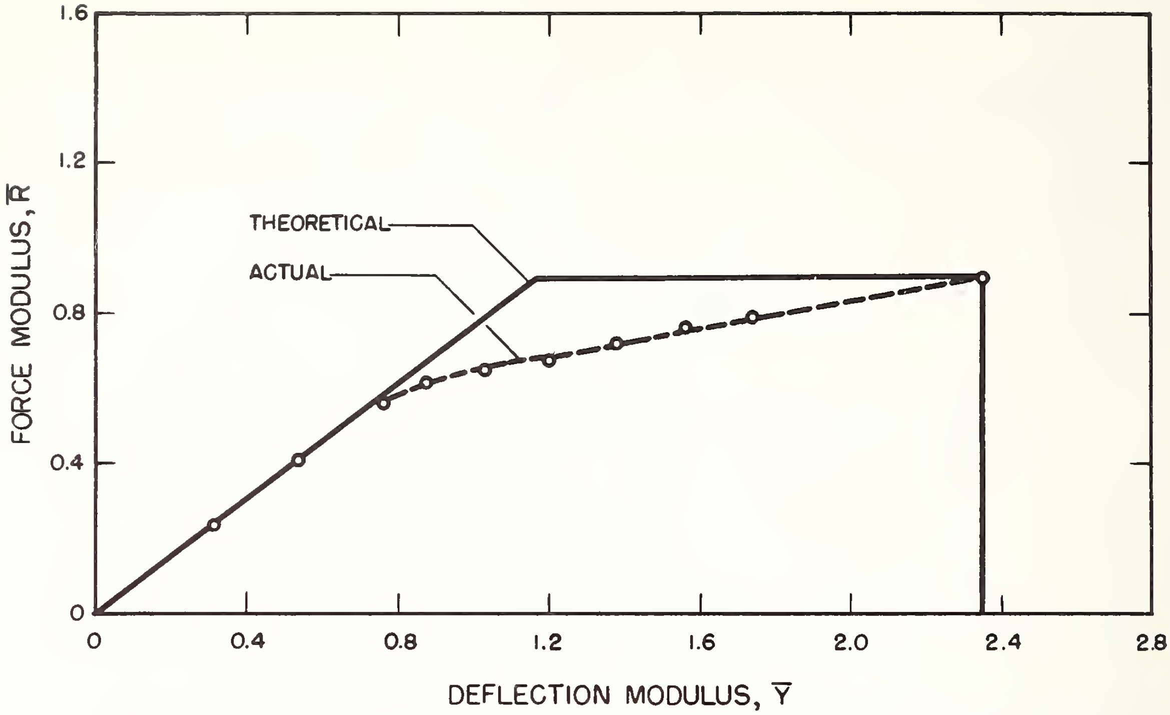

Figure 16.--Dimensionless force-deflection curve for tree stem No. TB-8, scarlet oak

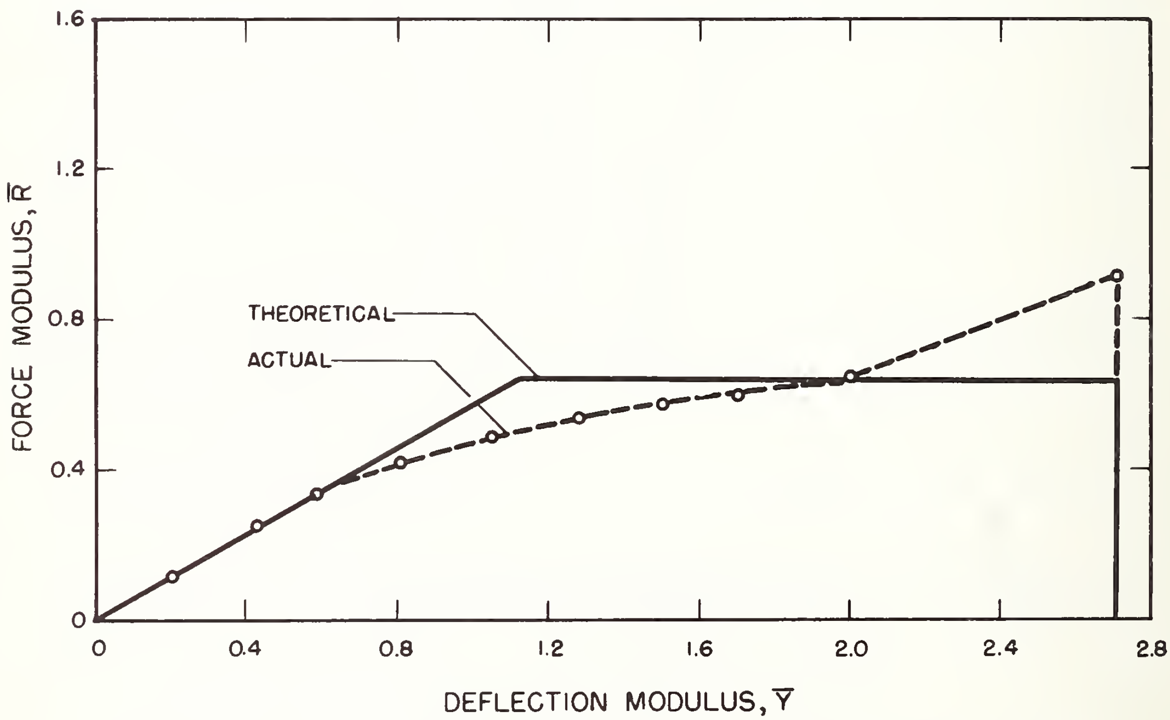

Figure 17.--Dimensionless force-deflection curve for tree stem No. TB-9, scarlet oak

Table 6.--Summary of statistical tests for homogeneity of sample population

Statistics	By species breaking			By species uprooting					
	S.O.[1]		Y.P.	S.B.		S.O.	S.B.+ S.O.		P.H.
Mean $\overline{E}_b$	1.551		1.412	1.384		1.290	1.330		1.214
Degrees of freedom		8			5			7	
Mean difference		.139			.094			.116	
Standard error of mean		.340			.508			.452	
Calculated Student's "t"		.409			.185			.257	
Tabular Student's "t" at 5%		2.360			2.571			2.365	

Statistics	By species											
	S.O.		Y.P.	S.O.+ Y.P.		S.B.	S.O.+ Y.P.+ S.B.		P.H.	S.O.+ Y.P.+ S.B.+ P.H.		A.B.
Mean $\overline{E}_b$	1.446		1.212	1.405		1.212	1.607		1.214	1.571		1.105
Degrees of freedom		13			17			19			21	
Mean difference		.234			.193			.393			.466	
Standard error of mean		.316			.310			.393			.252	
Calculated Student's "t"		.740			.622			1.000			1.849	
Tabular Student's "t" at 5%		2.160			2.110			2.093			2.080	

Statistics	Break and uproot failure			Normal and inflected failure		
	Break		Uproot	Normal		Inflected
Mean $\overline{E}_b$	1.409		1.303	1.324		1.421
Degrees of freedom		22			22	
Mean difference		.106			.097	
Standard error of mean		.211			.144	
Calculated Student's "t"		.503			.674	
Tabular Student's "t" at 5%		2.074			2.074	

1/ See key in table 1.

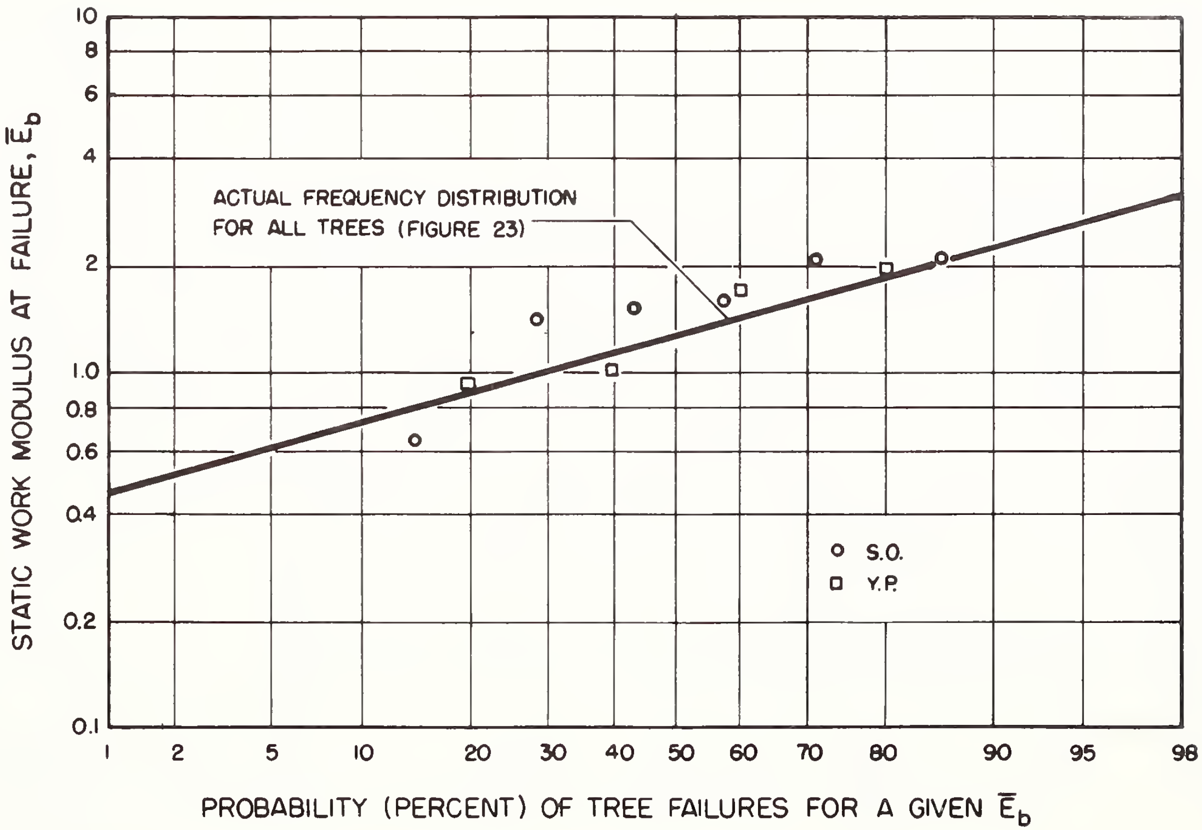

Figure 18.--Actual frequency distribution by species of static work moduli, $\overline{E}_b$, for trees breaking

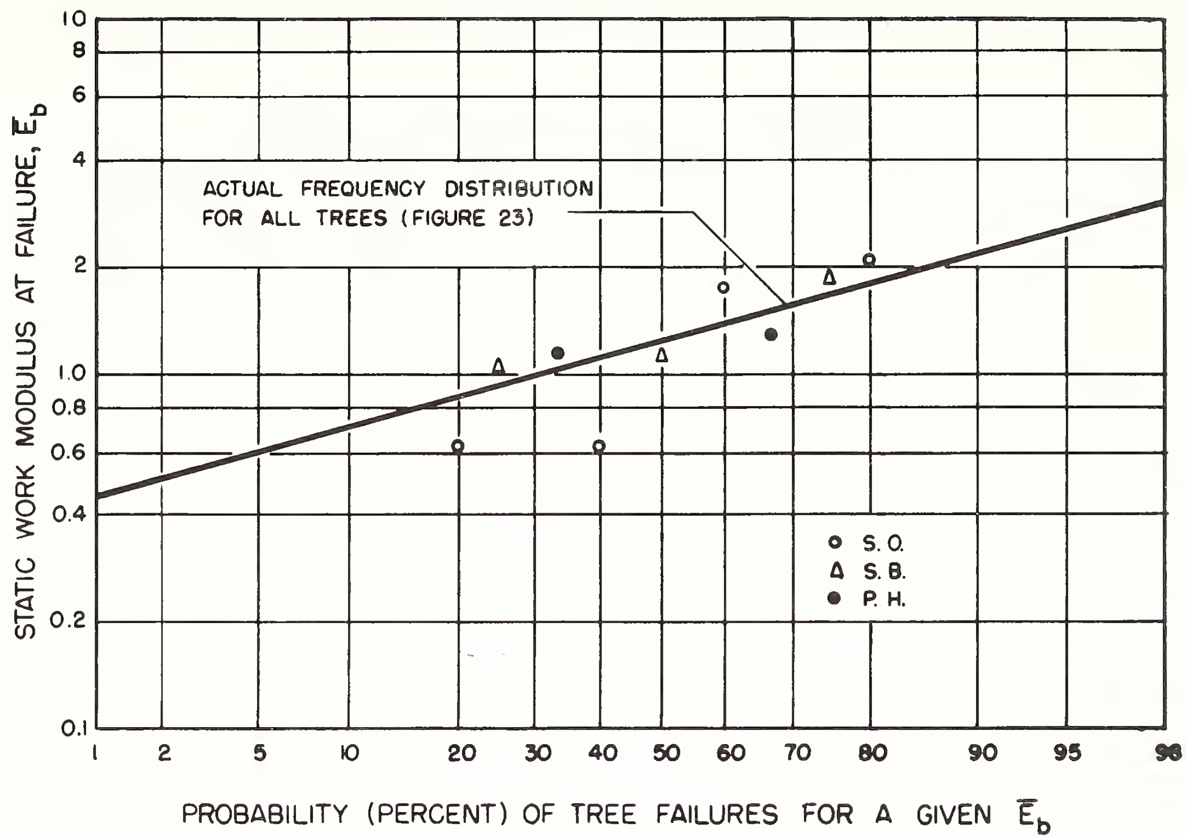

Figure 19.--Actual frequency distribution by species of static work moduli, $\overline{E}_b$, for trees uprooting

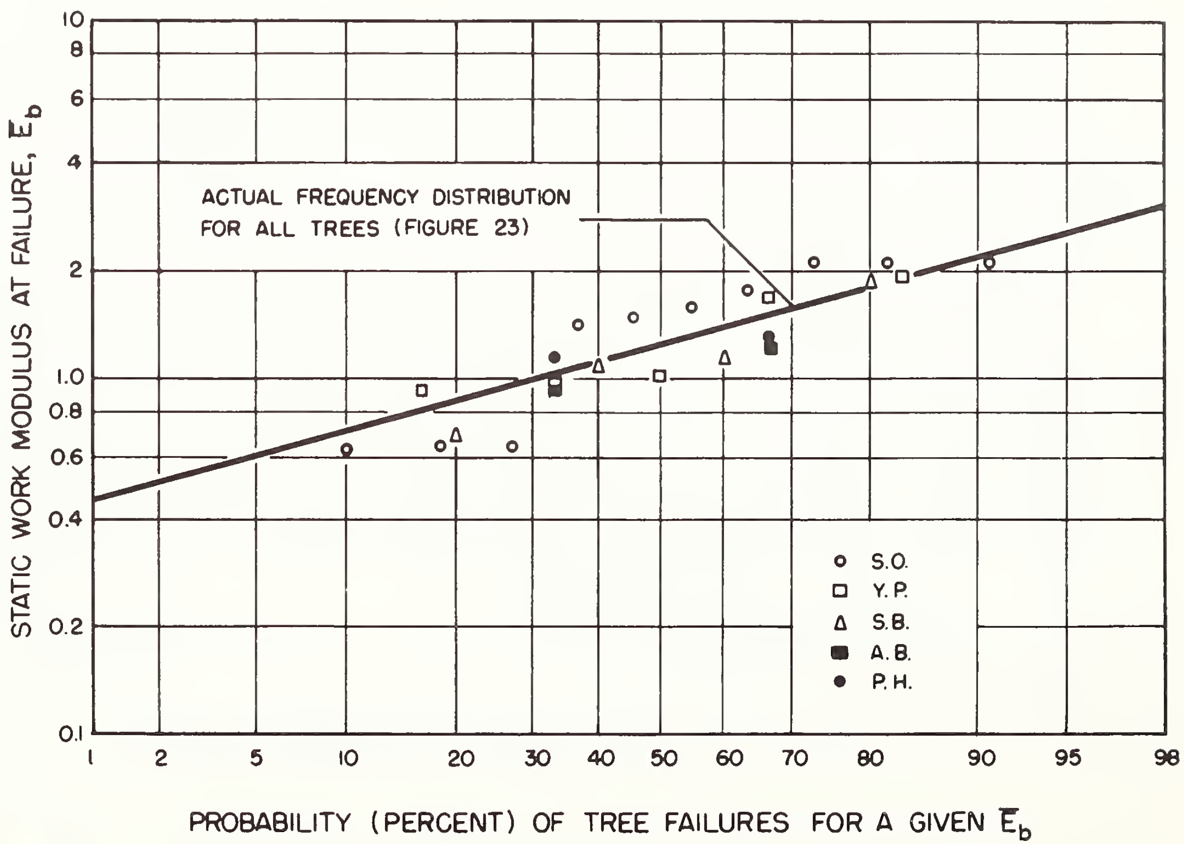

Figure 20.--Actual frequency distribution of static work moduli, $\overline{E}_b$, for different species

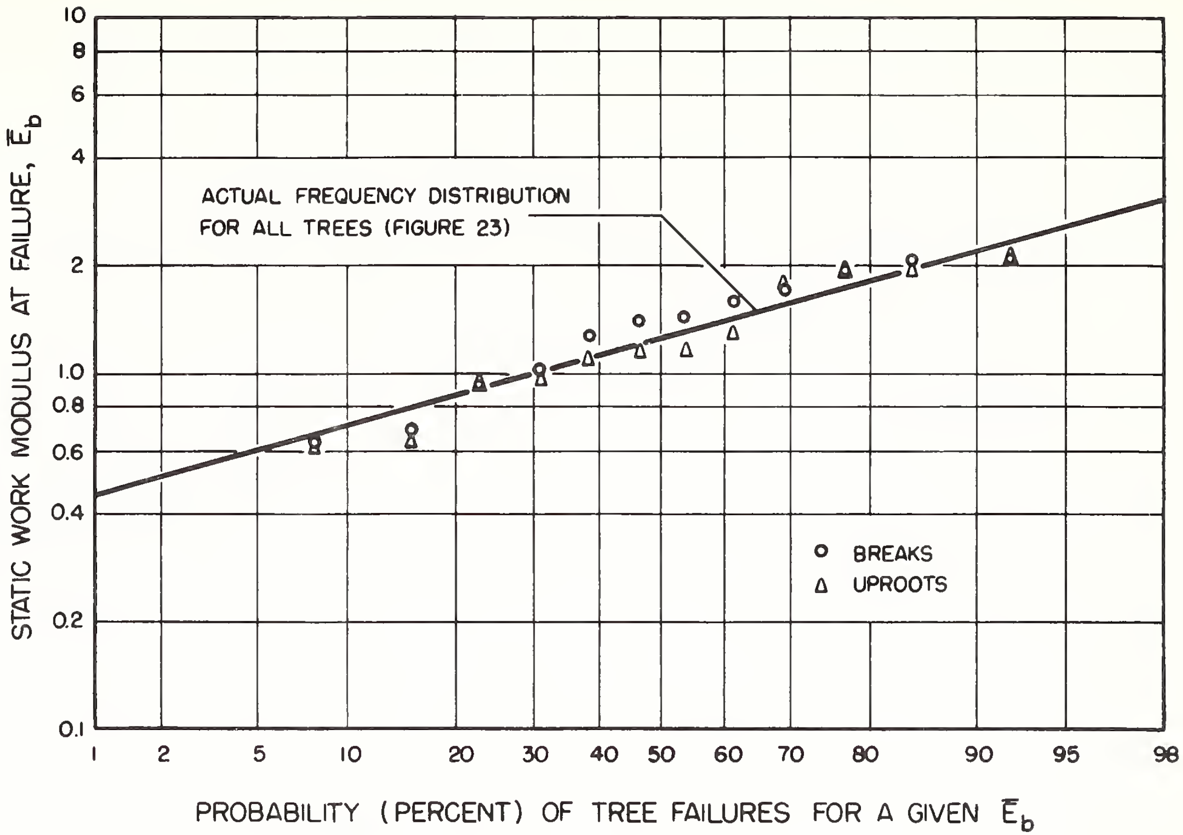

Figure 21.--Actual frequency distribution of static work moduli, $\overline{E}_b$, for breaks and uproots

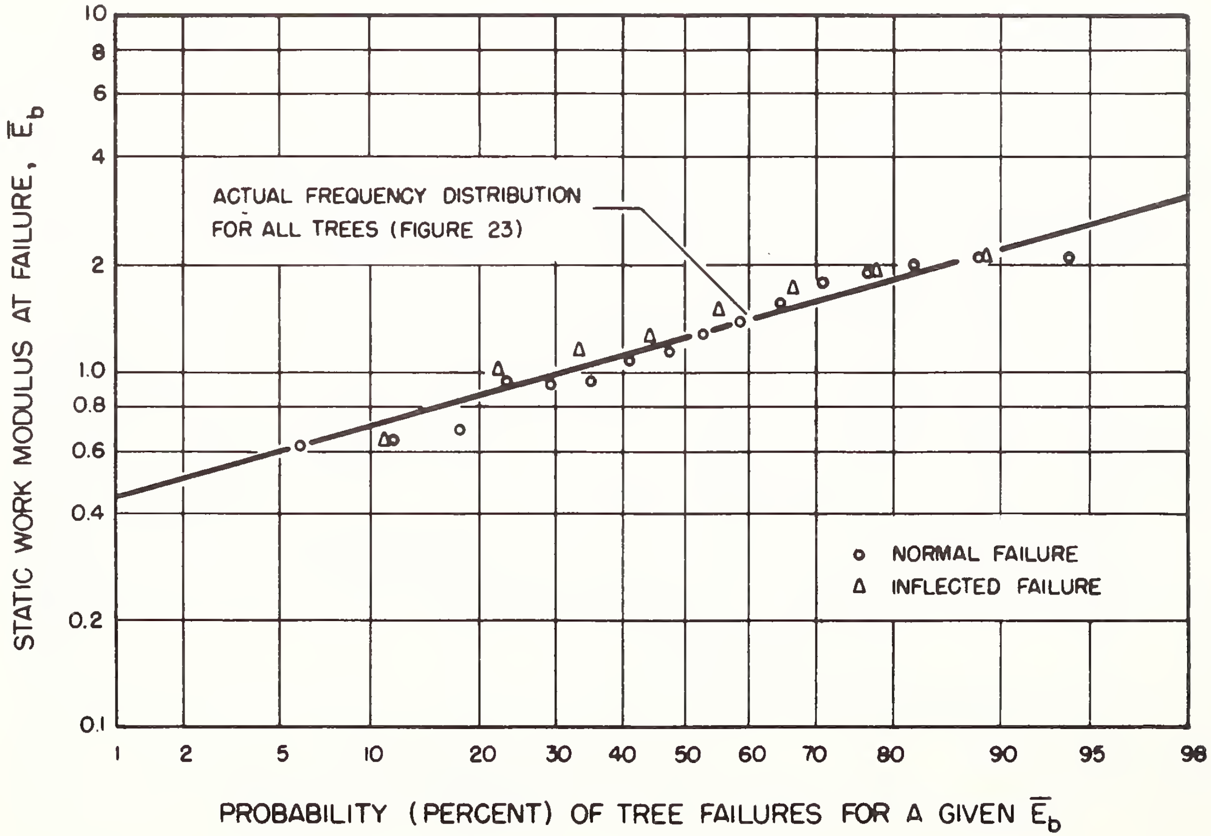

Figure 22.--Actual frequency distribution of static work moduli, $\overline{E}_b$, for normal and inflected failures

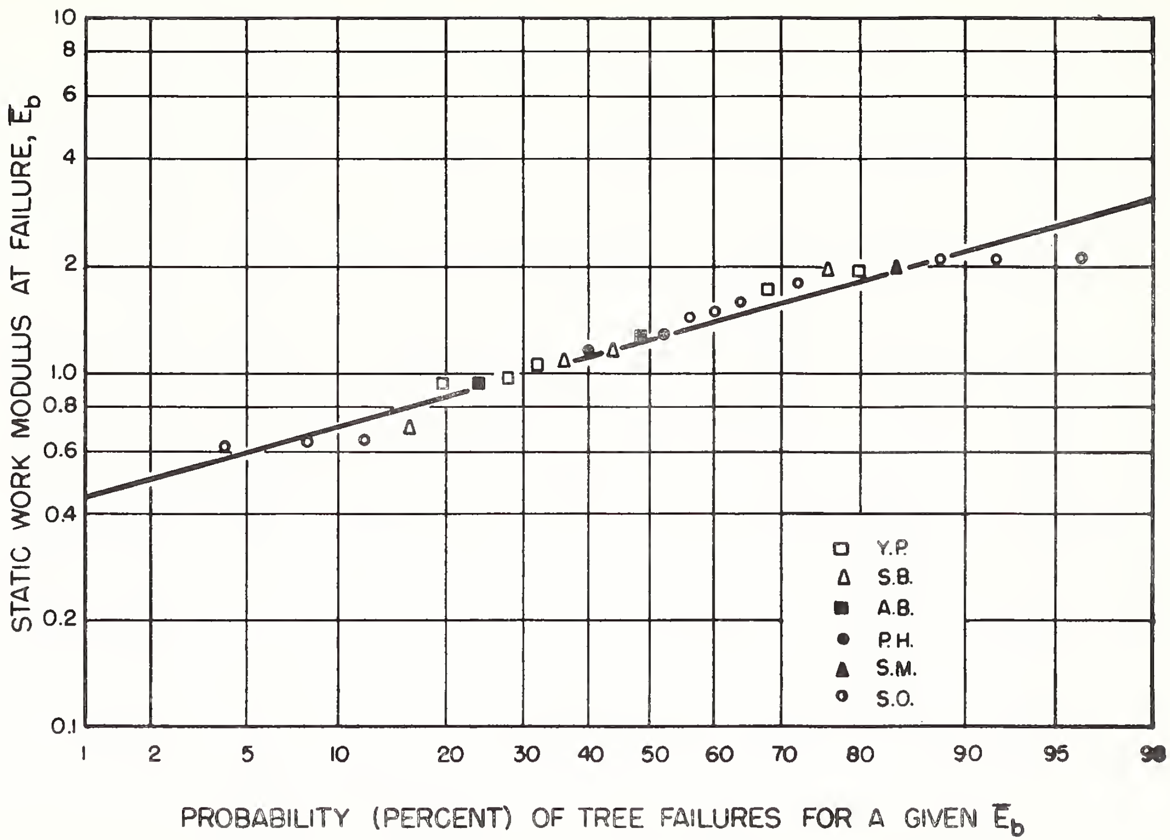

Figure 23.--Actual frequency distribution of static work moduli, $\overline{E}_b$, for all trees tested grouped into one sample population

The reference force R_r, for each tree stem was obtained by multiplying the theoretical restoring force constant, k_r, (equation (3)) by the reference deflection value, y_r.

Dimensionless values of the force modulus, $\bar{R}$, and the deflection modulus, $\bar{Y}$, at each interval of deflection and at failure were calculated by dividing R_e and y by the reference values R_r and y_r, respectively. Dimensionless force-deflection curves were then plotted using these values. Typical curves obtained in this study are presented in figures 16 and 17. Force-deflection moduli data for all trees tested are tabulated in Appendix B.

The static work modulus for breakage or uprooting, $\bar{E}_b$, was found by evaluating the area bounded by the theoretical force-deflection curve. Using parameters previously derived and presented in table 5

$$\bar{E}_b = \int_{\bar{Y}_o}^{\bar{Y}_b} \bar{R}d\bar{Y} \tag{12}$$

Expressing $\bar{R}$ in terms of $\bar{Y}$ and substituting into equation (12)

$$\bar{E}_b = \int_{\bar{Y}_o}^{\bar{Y}_1} (\bar{K}\ \bar{Y} + m)d\bar{Y} + \int_{\bar{Y}_1}^{\bar{Y}_b} (\bar{K}\ \bar{Y} + m)d\bar{Y} \tag{13}$$

where $\bar{Y}_1$ is the maximum deflection in the elastic region of the theoretical curve, and m is the ordinate intercept of the curve.

For statistical purposes of testing for homogeneity of the static work moduli, the values of $\bar{E}_b$ were grouped according to species and/or type of failure. Single values which could not be statistically tested were omitted from the groups involved. For those groups tested, differences between means were found not significant at the 5 percent level indicating the samples tested were drawn from a homogeneous population (table 6). Applying the chi-square test to the experimental values of $\bar{E}_b$ confirmed the hypothesis that the samples were also drawn from a normally distributed population.

Figures 18-23 present the actual frequency distributions of the static work moduli for the various groupings as percent of the cases occurring which are equal to or less than any chosen value of $\bar{E}_b$. As before, single values which could not be compared were not included in the distributions concerned.

DISCUSSION OF RESULTS

Because of the heterogeneous nature of wood, considerable variation in strength and other related properties are to be expected. Even when clear specimens are tested, the variation is surprisingly large (16).

When the force-deflection data gathered in this study were plotted, it was found that some of the trees exhibited curves with a definite inflection (figure 9) before failure by breaking or uprooting occurred. In some cases a steady drop in force (figure 10) was recorded before failure. These deviations from the normal type of curves (figures 8 and 11) can be explained in part, if not completely, by the base fixity of the trees in relation to their strength properties.

Fegel (9) who investigated the strength properties of trunk, branch, and root wood in certain northeastern trees, which, incidently, included some of the species studied in this report, found root wood to be much weaker in tension and compression than either trunk or branchwood. His results indicate, however, that root wood stressed in tension was approximately equal in strength to trunk wood stressed in compression. In addition, root wood was found to be approximately twice as strong in tension as it was in compression.

If a force of sufficient magnitude is applied to a tree such that the wood in the stem is stressed beyond the elastic limit, further loading may cause the roots to fail in compression. This was brought out by Mergen (12) in his paper on the mechanics of wind-breakage and windthrow. He emphasized the fact that the roots of a tree which is not firmly fixed at its base would fail in compression on the leeward side before the roots on the windward side are subjected to tension stresses. Depending on the tenacity, distribution, and strength of the roots on the tension (windward) side of the tree, variations in the form of the force-deflection curves can be expected. If the roots are quite firm when stressed in tension, an inflection in the curve will result. Whether the stem uproots or breaks after the inflection depends on the aggregate strength of the roots in comparison to the stem strength. If, on the other hand, the roots are not firm when stressed in tension, excessive root slippage will occur with a subsequent drop in force as the stem uproots. It is interesting to note that a drop in force can also occur when a stem is stressed to breakage. This is a result of compression failures forming along the stem as it is stressed.

It can be seem from the summary presented in table 4 that uprooting failures occurred in all species tested and breakage in all but two, pignut hickory and silver maple. Additional tests would have undoubtedly resulted in breakage failures for these two species also.

From the preceding discussion it is apparent that soil moisture plays an important role in determining the base fixity of the tree stem. Many workers have reported that excessive moisture in the soil coupled with poor drainage were important determinants in windthrow (1,7,8,12,15).

Throughout the summer of 1952, when the trees for this paper were tested, heavy periodic precipitation was encountered. There was, however, no noticeable difference in the frequency of uprooting during these periods. Good drainage in the clay type soil of the test area may partially explain this discrepancy.

For those trees that broke, position of breakage, f_{br}, was found to be near or at breast height (table 2). Stress at position of breakage calculated by equation (9) averaged lower for the different species than either the calculated maximum stress, S_m, or the modulus of rupture for green sawed specimens (table 3).

Differences in base fixity and structural irregularities in tree stems account for the major part of the variation in magnitude of the moduli $\overline{R}_b$, $\overline{Y}_b$, and $\overline{K}$. These irregularities include variations in mechanical properties of the wood due to differences in growth rate, specific gravity, and percentage of sapwood. The influence of sapwood on mechanical properties was demonstrated by Wakefield (17), who found the sapwood of yellow birch 27 percent stronger than heartwood in work to maximum load even though the heartwood averaged higher in modulus of rupture. Other irregularities, such as variations in soundness, stem form, injury, and knot distribution, also contribute to the variation of these three moduli.

Since the equation to calculate the static work modulus (equation (13)) does not delineate the force modulus at the proportional limit, nor define the elastic and plastic regions of the theoretical force-deflection curve, a constant force modulus in the plastic region was assumed. For the majority of the trees tested, the static work modulus was calculated using the maximum computed value of $\overline{R}$ as the constant force modulus (figure 16). Where a tree exhibited an inflection (figure 9), however, the static work modulus was based on the force modulus at the inflection (figure 17). Treating "inflection" trees in this manner was necessary in view of the fact that using the maximum $\overline{R}$ value would have resulted in $\overline{E}_b$ values much greater than the actual static work moduli of these trees.

The assumption that the force modulus is constant in the plastic region gave slightly higher values of $\overline{E}_b$ than was actually absorbed. This can be seen in comparing the actual curves with the theoretical curves in figures 16 and 17.

Although the method used to calculate the static work modulus does not take into account the energy of inflection exhibited by some of the trees, the $\bar{E}_b$ values presented in this paper have included this energy as part of the static work modulus. This was done after it was found that the energy of inflection was only a small part of the total static work modulus.

From table 6 it is apparent that some species were not included in the various groups segregated for statistical analysis. They were deleted because of a limited sample of trees taken for the various species and the occurrence of single values of $\bar{E}_b$ which could not be statistically evaluated for a specific group. Even with these limitations, however, the results indicate the trees for this study were from a homogeneous population and could be treated as a group.

The actual frequency distribution of the various groups of $\bar{E}_b$ values (figures 18-22) were plotted to determine whether species or type of failure had any affect on the energy level of failure for these groups in comparison to the actual frequency distribution of all trees tested, grouped into one sample population (figure 23). The greatest variance can be seen in figures 18-20, where the energy levels were approximately the same but the range of $\bar{E}_b$ values within a group showed large variations. A major part of these variations can be explained by the limited data collected for the various species. A larger sample would undoubtedly have given much better results.

From figures 21-22 it can be seen that the actual frequency distributions of $\bar{E}_b$ values of the various types of failures varied only slightly, and the energy levels were approximately the same in magnitude. This would seem to indicate that breakage and uprooting, with or without an inflection, require the same amount of energy.

It should be pointed out at this time that even though data for only one silver maple were collected in this study, the data were included in the distribution curve for all trees (figure 23). This decision was based on the value of the static work modulus calculated for this tree, which appeared to be of the same order of magnitude as that for the other species studied (see table 5).

From the frequency distribution curve of $\bar{E}_b$ values presented in figure 23, the energy required to break or uproot any given tree in a site II or better mixed-hardwood forest can be predicted for any probability level. The extent of damage that a site II or better-mixed hardwood forest may sustain for a given energy level can also be predicted. Based on the sample taken for this study, approximately one-half of the failures that will occur in this site-class will be by breaking.

CONCLUSIONS

1) Results of this study permit the prediction of the energy necessary to cause breakage and uprooting of hardwoods in a site II or better forest.

2) The extent of damage that may be sustained by this forest at a given energy level may also be predicted.

3) Based on the sample studied, approximately one-half of the failures that will occur will be by breaking.

4) The energy required to break or uproot hardwood trees is approximately equal.

5) The position of breakage for hardwood tree stems is at or near breast height.

6) Stress at position of breakage averaged lower than the calculated maximum stress.

7) Base fixity is a very important factor in determining whether failure is by breaking or uprooting.

APPENDIX A

EQUIVALENT FORCE AND CHORD-DEFLECTION FOR STATIC BENDING TEST

Table 7.--Equivalent force and chord-deflection for static bending test

Tree No.	Species		Equivalent force R_e (lbs) and chord-deflection y (ft)[1]							
TA-14	Y.P.	R_e	32	55	89	104	117	125	253	
		y	4.0	6.7	9.5	11.2	11.2	15.3	37.2	
TA-29	Y.P.	R_e	43	153	234	282	299	353		
		y	3.5	6.5	10.1	14.4	21.3	28.9		
TA-34	Y.P.	R_e	832	1471	2947	3264	3498	3632	3920	3825
		y	1.9	3.3	6.9	8.8	10.2	12.5	14.1	16.7
TA-35	Y.P.	R_e	304	599	798	830	819	894		
		y	3.7	7.9	12.5	15.8	18.8	23.0		
TA-37	Y.P.	R_e	457	713	943	1087	1367			
		y	5.6	9.1	13.1	16.8	26.0			
TA-23	S.B.	R_e	533	1031	1502	1860	2062	1920		
		y	2.6	4.2	7.8	10.0	12.5	16.6		
TA-31	S.B.	R_e	1483	1627	2626	2992	3076	3142		
		y	1.1	2.7	4.3	5.8	7.4	12.6		
TA-38	S.B.	R_e	215	492	770	1025	1273			
		y	2.1	4.3	6.1	9.9	23.3			
TA-39	S.B.	R_e	258	327	368	382	383	363		
		y	4.1	6.3	10.0	12.6	15.8	20.2		
TA-44	A.B.	R_e	148	288	356	406	435	467	524	
		y	3.1	6.7	9.7	12.1	14.7	17.8	21.1	
TA-45	A.B.	R_e	199	564	811	1006	1155	1196	1184	1208
		y	1.4	5.8	7.3	9.5	12.5	14.5	16.4	19.1
TA-22	P.H.	R_e	92	259	300	407	572	617	713	2117
		y	3.8	6.8	8.2	10.5	16.7	18.6	22.2	43.1

1/ Force and deflection in last column for each tree are values at failure.

Table 7 (continued)

Tree No.	Species		Equivalent force R_e (lbs) and chord-deflection y (ft)[1/]										
TA-33	P.H.	R_e	132	253	329	350	359	379	277				
		y	5.8	10.3	13.3	17.1	20.4	23.2	36.6				
TA-24	S.M.	R_e	825	2035	2527	2812	2785	2676					
		y	3.0	6.7	10.2	14.3	16.6	19.7					
TA-8	S.O.	R_e	1259	1655	1846	1795	1994						
		y	5.8	9.9	14.3	16.1	21.1						
TA-9	S.O.	R_e	1369	1643	1879	1969	2143	2395					
		y	4.2	7.1	11.5	15.3	18.6	21.8					
TB-1	S.O.	R_e	495	1010	965	1230	1294	1357	1410	1449			
		y	1.3	3.8	6.0	8.7	11.2	13.8	16.4	20.8			
TB-2	S.O.	R_e	206	610	880	1145	1242	1353	1525				
		y	3.0	6.0	8.4	9.8	12.6	14.9	23.3				
TB-3	S.O.	R_e	190	482	700	1194	1243	1357	1387				
		y	3.0	6.2	10.3	13.6	16.6	20.5	28.6				
TB-4	S.O.	R_e	655	814	1041	1127	1179	1196	1091	1115	1025		
		y	5.5	7.8	10.5	13.3	15.7	22.4	26.6	29.2	39.4		
TB-5	S.O.	R_e	119	155	907	937	985	997	1024	1030	1103	1255	1773
		y	6.0	10.2	14.0	17.0	19.9	22.6	26.1	29.5	33.0	39.0	42.8
TB-6	S.O.	R_e	242	566	733	987	1112	1204	1286				
		y	4.6	6.8	8.3	12.2	14.7	16.5	24.8				
TB-8	S.O.	R_e	523	918	1241	1353	1439	1492	1602	1688	1746	1981	
		y	4.0	7.0	9.8	11.3	13.3	15.5	17.8	20.2	22.5	30.4	
TB-9	S.O.	R_e	421	906	1207	1519	1749	1955	2055	2175	2340	3320	
		y	2.6	5.5	7.4	10.1	13.2	16.3	19.0	21.8	25.6	34.2	

1/ Force and deflection in last column for each tree are values at failure.

APPENDIX B

FORCE MODULUS AND DEFLECTION MODULUS FOR STATIC BENDING TEST

Table 8.--Force modulus and deflection modulus for static bending test

Tree No.	Species		Force modulus $\bar{R}$ and deflection modulus $\bar{Y}$[1]							
TA-14	Y.P.	$\bar{R}$	.172	.296	.483	.559	.624	.669	1.351	
		$\bar{Y}$	.256	.429	.608	.717	.717	.981	2.384	
TA-29	Y.P.	$\bar{R}$	.085	.303	.463	.558	.529	.701		
		$\bar{Y}$	.265	.492	.769	1.090	1.613	2.189		
TA-34	Y.P.	$\bar{R}$	.137	.242	.485	.538	.576	.598	.645	.630
		$\bar{Y}$	.232	.402	.841	1.073	1.244	1.524	1.720	2.036
TA-35	Y.P.	$\bar{R}$	.302	.594	.792	.823	.812	.887		
		$\bar{Y}$	.456	.975	1.543	1.951	2.321	2.839		
TA-37	Y.P.	$\bar{R}$	.239	.374	.495	.571	.717			
		$\bar{Y}$	.421	.684	.985	1.263	1.954			
TA-23	S.B.	$\bar{R}$	.182	.353	.514	.637	.706	.657		
		$\bar{Y}$	.226	.365	.678	.869	1.086	1.443		
TA-31	S.B.	$\bar{R}$	.318	.349	.564	.643	.661	.676		
		$\bar{Y}$	.186	.457	.728	.983	1.254	2.135		
TA-38	S.B.	$\bar{R}$	.096	.221	.347	.461	.573			
		$\bar{Y}$	.184	.377	.535	.868	2.044			
TA-39	S.B.	$\bar{R}$	.487	.618	.696	.722	.725	.685		
		$\bar{Y}$	.603	.927	1.471	1.854	2.325	2.972		
TA-44	A.B.	$\bar{R}$	.284	.550	.680	.775	.830	.891	.998	
		$\bar{Y}$	.317	.686	.992	1.239	1.504	1.823	2.168	
TA-45	A.B.	$\bar{R}$	.120	.340	.488	.605	.696	.720	.712	.727
		$\bar{Y}$	.143	.591	.743	.968	1.272	1.475	1.670	1.945
TA-22	P.H.	$\bar{R}$	.067	.190	.219	.298	.419	.452	.522	1.550
		$\bar{Y}$	.148	.265	.320	.410	.652	.726	.867	1.683

1/ Moduli in last column for each tree are values at failure.

Table 8 (continued)

Tree No.	Species		Force modulus $\overline{R}$ and deflection modulus $\overline{Y}$[1/]										
TA-33	P.H.	$\overline{R}$	.122	.235	.305	.325	.333	.352	.257				
		$\overline{Y}$	.592	1.051	1.357	1.744	2.081	2.367	3.734				
TA-24	S.M.	$\overline{R}$	.280	.690	.858	.954	.945	.908					
		$\overline{Y}$	.432	.965	1.469	2.060	2.392	2.838					
TA-8	S.O.	$\overline{R}$	.436	.574	.640	.672	.691						
		$\overline{Y}$	.716	1.222	1.765	1.987	2.604						
TA-9	S.O.	$\overline{R}$	.331	.397	.465	.488	.518	.579					
		$\overline{Y}$	.224	.379	.614	.818	.994	1.165					
TB-1	S.O.	$\overline{R}$	.102	.228	.201	.256	.269	.282	.293	.301			
		$\overline{Y}$	.147	.427	.674	.977	1.258	1.550	1.843	2.337			
TB-2	S.O.	$\overline{R}$	.075	.223	.321	.418	.453	.494	.557				
		$\overline{Y}$	.208	.416	.583	.681	.875	1.034	1.618				
TB-3	S.O.	$\overline{R}$	.126	.321	.467	.796	.829	.905	.925				
		$\overline{Y}$	.341	.704	1.170	1.545	1.886	2.329	3.250				
TB-4	S.O.	$\overline{R}$	.302	.376	.481	.520	.544	.552	.504	.515	.473		
		$\overline{Y}$	.514	.729	.981	1.243	1.467	2.093	2.486	2.729	3.682		
TB-5	S.O.	$\overline{R}$	.081	.105	.617	.637	.670	.678	.696	.701	.750	.853	1.206
		$\overline{Y}$	.480	.816	1.120	1.320	1.592	1.808	2.088	2.360	2.640	3.120	3.424
TB-6	S.O.	$\overline{R}$	.169	.393	.509	.686	.772	.836	.894				
		$\overline{Y}$	.605	.895	1.092	1.605	1.934	2.171	3.263				
TB-8	S.O.	$\overline{R}$	.236	.415	.561	.611	.650	.674	.724	.763	.789	.895	
		$\overline{Y}$	.308	.540	.756	.871	1.025	1.195	1.372	1.557	1.735	2.344	
TB-9	S.O.	$\overline{R}$	.116	.250	.333	.419	.482	.539	.567	.600	.645	.916	
		$\overline{Y}$	.206	.436	.587	.801	1.047	1.293	1.507	1.730	2.031	2.714	

1/ Moduli in last column for each tree are values at failure.

LITERATURE CITED

1. Anderson, K.F.
   1954. Gale and wind damage to the forests, with special reference to the effects on the storm of 31st January 1953, in the northeast of Scotland. Forestry 27(2):97-121. 57 ref., illus.

2. Behre, C. E.
   1921. A study of windfall in the Adirondacks. Jour. For. 19(6): 632-637.

3. ______
   1927. Form-class taper curves and volume tables and their application. Jour. Agric. Res. 35(8):673-744. 27 ref., illus.

4. Cajander, E. K.
   1934. [Observations in wind damage in Finland.] Acta Forestalia Fennica 40:251-269. [Transl. No. 83, Div. Silvics, U.S. Forest Service, 4pp., Processed.]

5. Clapp, R. T.
   1938. The effects of the hurricane upon New England forests. Jour. For. 36(12):1177-1181.

6. Curtis, J. D.
   1943. Some observations on wind damage. Jour. For. 31(12):877-882. 12 ref., illus.

7. Day, W. R.
   1950. The soil conditions which determine windthrow in forests. Forestry 23(2):90-95. 3 ref.

8. ______
   1953. The growth of sitka spruce on shallow soils in relation to root-disease and wind throw. Forestry 26(2):81-95. 3 ref., illus.

9. Fegel, A. C.
   1941. Comparative anatomy and varying physical properties of trunk, branch, and root wood in certain northeastern trees. The New York State College of Forestry. Tech. pub. No. 55. 20 pp., 13 ref.

10. Fons, W. L.
    1953. Tree breakage characteristics under static loading, ponderosa pine, AFSWP-406, Confidential. U.S. Forest Service, Div. of Fire Research. 45 pp., illus.

11. Markwardt, L. J., and Wilson, T. R. C.
1935. Strength and related properties of woods grown in the United States. Tech. Bull. 479, U. S. Dept. Agric., For. Prod. Lab., 99 pp., 61 ref., illus.

12. Mergen, F.
1954. Mechanical aspects of wind-breakage and windfirmness. Jour. For. 52(2):119-125. 16 ref., illus.

13. Sauer, F. M., Fons, W. L., and Storey, T. G.
1954. Blast damage to coniferous tree stands by atomic explosions, WT-731, Confidential-Restricted Data. U. S. Forest Service, Div. of Fire Research, 84 pp., illus.

14. Sherlock, R. H., et al
1936. Storm loading and strength of wood pole lines and a study of wind gusts. 183 pp., illus. Easton, Pa.

15. Smith, D. M.
1946. Storm damage in New England forests. Masters thesis, 173 pp., 114 ref., illus. Yale Univ.

16. Stern, G. E.
1947. Influence of nonhomogeneity of wood on its strength properties. A.S.T.M. preprint, 8 pp., 7 ref., illus.

17. Wakefield, W. E.
1937. A comparison of the mechanical and physical properties of the heartwood and sapwood of yellow birch. Dept. of Mines and Resources, Canada. For. Serv. Cir. 51, 8 pp., illus.

NOMENCLATURE

The following nomenclature is used in the paper:

a = constant in stem-form equation

b = constant in stem-form equation

$c = \frac{b}{a}$, stem-form factor

d = diameter along stem inside bark, in.

d_{bh} = stem diameter at breast height, in.

d_i = stem diameter inside bark at breast height, in.

E = modulus of elasticity, lbs/sq. in.

$\bar{E}_b$ = static work modulus at failure

$f = H/H_{bh}$, fractional height of stem measured from top of stem downward

f_{br} = position of stem breakage

f_m = position of maximum stress

f_l = position of loading

H = height of stem measured from top of stem downward, ft

H_{bh} = height of stem above breast height, ft

H_{cp} = height of stem above breast height to loading point, ft

H_o = total height of tree from ground, ft

I_i = moment of inertia inside bark at breast height, in.

k_a = actual restoring force constant, lbs/ft

k_r = theoretical restoring force constant, lbs/ft

L = moment arm

$\bar{K} = k_a/k_r$, restoring force constant modulus

MR = modulus of rupture, lbs/sq in.

$Q_{f_1} = \left(\frac{32R_{eb} H_{bh}}{\pi d_i^3} \right)_{f_1}$, stress function at f = 1

R_a = actual force, lbs

R_e = equivalent force, lbs

R_{eb} = equivalent force at failure, lbs

R_r = reference force, lbs

$\overline{R} = R_e/R_r$, force modulus

$\overline{R}_b = R_{eb}/R_r$, force modulus at failure

S = extreme fiber stress, lbs/sq. in.

S_{bh} = extreme fiber stress at breast height, lbs/sq. in.

S_{br} = extreme fiber stress at position of stem breakage, lbs/sq. in.

S_m = maximum extreme fiber stress, lbs/sq. in.

y = stem deflection at point of loading, ft

y_b = deflection at failure, ft

y_r = reference deflection, ft

$\overline{Y} = y/y_r$, deflection modulus

$\overline{Y}_b = y_b/y_r$, deflection modulus at failure

$z = d/d_{bh}$, ratio of diameter of stem to diameter at breast height

$\overline{\beta} = \frac{k_r H^3_{bh}}{3EI_i}$, restoring force function

δ_m = maximum strain, in./in.

δ_r = reference strain, μ in./in.

ψ = a function

INITIAL
DISTRIBUTION LIST FOR
AFSWP-970

ADDRESSEE	NO OF CYS
ARMY	
Chief of Research and Development, D/A, Washington 25, D. C. ATTN: Atomics, Air Defense and Missile Division	1
Chief of Engineers, D/A, Washington 25, D. C. ATTN: ENGNB	1
ATTN: ENGEB	1
Commanding General, Continental Army Command, Ft. Monroe, Va.	1
President, Board #4, Headquarters, CONARC, Ft. Bliss, Tex.	1
Commander-in-Chief, FECOM, APO 500, San Francisco, C lif. ATTN: ACofS, J-3	2
Commandant, Command and General Staff College, Ft. Leavenworth, Kans. ATTN: ALLLS (AS)	1
Director, Special Weapons Development Office, Headquarters, CONARC, Ft. Bliss, Texas	1
Commanding General, The Engineer Center, Ft. Belvoir, Va. ATTN: Asst. Commandant, Eng. School	1
Commanding Officer, Chemical and Radiological Lab, Army Chemical Center, Md. ATTN: Tech Library	1
Commanding Officer, Transportation R and D Command, Ft. Eustis, Va. ATTN: Special Projects Division	1
Director, Operations Research Office, Johns Hopkins University, 7100 Connecticut Avenue, Chevy Chase, Md., Washington 15, D.C.	1
Chief of Ordnance, D/A, Washington 25, D. C. ATTN: ORDTX-AR	1
NAVY	
Chief of Naval Operations, D/N, Washington 25, D.C. ATTN: OP-36	2
Chief of Naval Operations, D/N, Washington 25, D.C. ATTN: OP-03EG	1
Director of Naval Intelligence, D/N, Washington 25, D.C. ATTN: OP-922V	1
Chief of Naval Research, D/N, Washington 25, D.C. ATTN: Code 811	1

INITIAL
DISTRIBUTION LIST
FOR AFSWP-970

ADDRESSEE	NO OF CYS
NAVY (Continued)	
Commandant of the Marine Corps, D/N, Washington 25, D.C. ATTN: Code A03H	4
President, U.S. Naval War College, Newport, R.I.	1
Superintendent, U.S. Naval Postgraduate School, Monterey, Calif.	1
Commanding Officer, U.S. Naval Schools Command, U.S. Naval Station, Treasure Island, San Francisco, Calif.	1
Commanding Officer, U.S. Fleet Training Center, Naval Base, Norfolk 11, Va. ATTN: Special Weapons School	1
Commanding Officer, U.S. Fleet Training Center, Naval Station, San Diego, Calif. ATTN: SPWP School	2
Commanding Officer, Air Development Squadron 5, VX-5, U.S. Naval Air Station, Moffett Field, Calif.	1
Commanding Officer, U.S. Naval Damage Control Training Center, Naval B se, Philadelphia, Pa. ATTN: ABC Defense Course	1
Officer-in-Charge, U.S. Naval Civil Engineering Research and Evaluation Laboratory, U.S. Naval Construction Bn. Center, Port Hueneme, Calif. ATTN: Code 753	1
Director, U.S. Naval Research Lab., Washington 25, D. C.	1
AIR FORCE	
Assistant for Atomic Energy, Headquarters, USAF, Washington 25, D.C.	1
Director of Plans, Headquarters, USAF, Washington 25, D.C. ATTN: War Plans Division	1
Director of Research and Development, Headquarters, USAF, Washington 25, D.C. ATTN: Combat Components Division	1
Director of Requirements, Headquarters, USAF, Washington 25, D.C. ATTN: AFDRQ-SA/M	1
Director of Intelligence, Headquarters, USAF, Washington 25, D.C. ATTN: AFOIN-1B2	1
Commander, Air Research and Development Command, P.O. Box 1395, Baltimore 3, Md. ATTN: RDDN	1
Director, Air University Library, Maxwell AFB, Ala.	2

INITIAL
DISTRIBUTION LIST
FOR AFSWP-970

ADDRESSEE	NO OF CYS
AIR FORCE (Continued)	
Commander, Wright Air Development Center, Wright-Patterson AFB, Ohio ATTN: WCOSI	1
Commander, AF Cambridge Research Center, L.G. Hanscom Field, Bedford, Mass. ATTN: CRQST-2	1
Commander, AF Special Weapons Center, Kirtland AFB, N.M. ATTN: Library	1
Commandant, USAF Institute of Technology, Wright-Patterson AFB, Ohio ATTN: Resident College	1
Commander, 1009th Special Weapons Squadron, Headquarters, USAF, Washington 25, D.C.	1
The RAND Corporation, 1700 Main Street, Santa Monica, California (For Nuclear Energy Division)	1
Assistant Chief of Staff, Installations, Headquarters, USAF, Washington 25, D.C. ATTN: AFCIE-E	1
OTHER DOD AGENCIES	
Assistant Secretary of Defense, (Research and Development), Washington 25, D.C. ATTN: Tech Library	1
U.S. Documents Officer, Office of the United States National Military Representative, SHAPE, APO 55, New York, N.Y.	1
Director, Weapons Systems Evaluation Group, OSD, Washington 25, D.C.	1
Commandant, Armed Forces Staff College, Norfolk 11, Va. ATTN: Secretary	1
Commander, Field Command, AFSWP, P.O. Box 5100, Albuquerque, N.M.	1
Commander, Field Command, AFSWP, P.O. Box 5100, Albuquerque, N.M. ATTN: Training Division	2
Chief, Armed Forces Special Weapons Project, Washington 25, D.C.	5
ASTIA, Document Service Center, UB Building, Dayton 2, Ohio ATTN: DCS-SA	4
OTHER	
A. A. Brown, Chief, Division of Forest Fire Research, Forest Service, U.S. Dept. of Agriculture, Washington 25, D.C.	10
British Joint Services Mission c/o A. A. Brown, Chief, Div. of Forest Fire Research Forest Service, U.S. Dept. of Agriculture, Washington 25, D.C.	1